Aerobic Selective Oxidation of Alcohols and Alkanes over Hydroxyapatite-Based Catalysts

Guylène Costentin, Franck Launay

Chapter 6. Aerobic Selective Oxidation of Alcohols and Alkanes over Hydroxyapatite-Based Catalysts

Guylène Costentin[1,*], *Franck Launay*[1]

Affiliation

[1] Sorbonne Université, CNRS, Laboratoire de Réactivité de Surface (LRS), 4 place Jussieu, 75005 Paris, France

* Dr Guylène Costentin, corresponding author
guylene.costentin@sorbonne-universite.fr

Keywords: selective oxidation, benzyl alcohol oxidation, methane, propane, oxidative dehydrogenation, metal dispersion, apatite stoichiometry.

Abstract:

Selective oxidation catalysis is of prime importance for the production of many key intermediates. The control of selectivity in the presence of gaseous oxygen is quite challenging and requires the development of efficient catalysts. Thanks to their large composition range, resulting from the modulation of their stoichiometry and substitution ability, hydroxyapatites can be modified by many metals which make them original catalytic systems gathering both tunable acid-base properties and redox properties. In this chapter, we will show the interest of metal modified hydroxyapatite catalysts for various classes of oxidation reactions. Due to their large range of stability, they can be implemented either in liquid phase for aerobic oxidation of alcohols (Pd, Ru), or at very high temperature (> 600°C) for gas phase alkane oxidation, partial oxidation of methane (Rh, Ni) and oxidative dehydrogenation of other alkanes (V, Co…). The influence of the metal incorporation method (ion exchange, impregnation in excess of solution, or coprecipitation) on the metal dispersion and catalytic performance will be discussed. Finally, the role of the basic properties of hydroxyapatites in the alkane activation will be discussed.

1. Introduction

Selective oxidation catalysis plays a crucial role in the current chemical industry for the production of many key intermediates. In particular, aldehydes and ketones can be obtained from primary or secondary alcohols. Despite oxygen activation remains challenging, selective aerobic alcohol oxidation is very attractive. In addition, in the context of decay of oil supplies, there is a renewed interest in light C1-C3 alkane valorisation. The proven reserves in natural gas are abundant, which makes this energy source available and quite cheap. Alkanes are also formed in large quantities by coal- and gas-to-liquid (CTL and GTL) plants. Partial oxidation of methane (POM) is a promising route for syngas production ($CH_4 + 1/2\ O_2 \rightarrow CO + 2H_2$). Similarly, given the increasing demand in olefins, there is a renewed interest for oxidative dehydrogenation (ODH) of $C \geq 2$ alkanes ($C_nH_{2n+2} + 1/2\ O_2 \rightarrow C_nH_{2n} + H_2O$).

For all these classes of selective oxidation reactions operating in the presence of oxygen, the optimization of selectivity should contribute to the establishment of novel green and sustainable chemical processes. It remains however quite challenging to avoid overoxidation, and the development of selective heterogeneous catalysts remains an important issue. Their formulations are mainly based on transition metal ions (TMI). Depending on the nature of the molecule to be selectively oxidized, different TMI are used either in their cationic or zerovalent form. Cu, Ru, Pd, Au, Fe, V, Ir, Os or Co are commonly used for the selective oxidation of alcohols [1]. Zerovalent Rh and Ni have been studied for the partial oxidation of methane [2-4]. In the case of C≥2 alkane oxidative dehydrogenation reactions, numerous TMI were used, alone or in combination [5] to form reducible oxides [6-8], nanostructured oxides [9] or isolated species [10], and V-based catalysts are the most extensively investigated for propane activation [11]. Beside the nature of TMI, its dispersion is a key parameter to control the selectivity. One can discriminate two classes of catalysts, bulk catalysts containing the TMI in its host lattice or metal supported catalysts. In the latter case, the nature of the carrier has been found to influence the performance of the system, due to its impact on the metal dispersion, but also due to the role played by the acid base properties on the adsorption-desorption of reactants and products. It was also found that the addition of phosphorus to Cr/TiO_2 and V_2O_5/TiO_2 improves the performance of various catalysts in the oxidative dehydrogenation of ethane (ODHE) or propane (ODHP) [12-14]. Several explanations for such beneficial role of phosphorus were proposed, such as appearance on the carrier of a new phosphate with adequate structure of active sites, isolation of active site (in contrast to promotion of total oxidation over oxide-like catalysts) and / or the tuning of the surface acid–base properties [15-18]. Among the

investigated phosphate compounds, $(VO)_2P_2O_7$ was identified as the active phase for the selective oxidation of n-butane to maleic anhydride [19] and many other iron [15, 20], molybdenum [21] and vanadium phosphate phases [22-24] were also investigated. In this context, the hydroxyapatite system (HA) was also studied from the 90's, since, depending on the strategy of synthesis, it can be advantageously used as a tunable carrier to get metal supported hydroxyapatite or directly as metal modified bulk catalyst thanks to the various substitution afforded by its flexible network. As developed in chapter 3 of this book, the stability of hydroxyapatite both in solution and at high temperature makes this system ideal for use in selective oxidation of alcohols operating in liquid phase and for high temperature gas phase reactions required for alkane activation. Its acid–base properties can also be tuned both by controlling the stoichiometry and by modifying its composition, especially going from calcium hydroxyapatite to strontium hydroxyapatite to favor basicity, eventually counterbalancing the acidity induced by TMI deposition. The great modulation of composition by substitution on both its cationic and anionic sites offers endless opportunities to get metal modified systems. Several strategies are used to incorporate transition metal ions, one pot coprecipitation syntheses likely to modify the bulk (and surface) properties to favor high metal dispersion, or more classical metal surface deposition onto the hydroxyapatite carrier. Such two-step approach includes impregnation or cationic exchanges. Both are performed in excess of solution and mainly differ by the absence of a washing step in the former case. As a result, the metal loading and the metal dispersion may differ to a large extent.

Given their key impact for the control of reactivity in the selective oxidation reactions, these aspects will be considered in this chapter. In a first section, the performances and key parameters governing the oxidation of alcohols will be reviewed. In a second section dedicated to gas phase reactions, results and main conclusions obtained from methane partial oxidation then oxidative dehydrogenation of propane, ethane, heptane and n-octane will be developed.

2. Liquid phase reactions: selective aerobic oxidative of alcohols

Aldehydes and ketones are key-compounds that can be obtained from primary and secondary alcohols. Oxidants, such as oxides (Cr, Mn, Ru), halides, peroxides or ozone, have been traditionally used for these reactions but they are often pointed out to be not environment friendly [25]. Guided by sustainable development, efforts have been made over the years to replace Cr reagents, particularly in medicinal chemistry and, the most popular oxidants are right

now either stoichiometric reagents such as Dess Martin periodinane (IBX), the Swern reagent or combinations of a terminal oxidant with a catalyst such as *N*-methyl morpholine-N-oxide (NMO) and TPAP or sodium hypochlorite and TEMPO [26]. In parallel, recent researches have led to an exponential increase in the number of publications dealing with combinations of O_2 (or H_2O_2) with homogeneous, heterogeneous catalysts or biocatalysts that afford a good atom economy and only water as a by-product but none of these systems has replaced yet those mentioned before in synthetic organic chemistry [27-29]. Dioxygen deserves special attention due to its natural availability but its activation is more challenging than that of H_2O_2 [30]. Catalytic systems working at low pressure as well as under mild reaction conditions and with a good selectivity and functional group tolerance are needed. Low catalyst loadings and the avoidance of costly or toxic additives are required too.

In this context, liquid phase apatite-based heterogeneous catalysts working with oxygen and involving mainly Ru or Pd have been explored. The different available systems tested in batch conditions will be compared considering benzyl alcohol (BA) as a model substrate. Their performance towards other primary and secondary alcohols, activated or not, will also be discussed. Information on the mechanism will be given using, if possible, *in situ* characterization of catalysts or experiments allowing the determination of Hammet constants or of the Kinetic Isotope Effect (K.I.E).

2.1 Apatite-based catalysts efficient in the aerobic oxidation of alcohols

Apatite is not an oxidation catalyst by itself. It must be combined with a transition metal. The main catalytic systems based on apatite developed for the oxidation of alcohols by oxygen reported since 2000 are presented in **Table 1** [31-40]. At best, we have tried to highlight the quantities of metal involved in the catalytic tests in order to be able to compare the performance of the catalysts with each other. The situation varies greatly from one article to another. Some authors do not give any information on the TOF values, or if they do, the TOFs are measured either over the whole reaction or at the lowest conversion values, which is normally more favorable. Historically, the first example dates back to the work of Kaneda *et coll.* (**Table 1**, entry 1) [31]. One of the most common reasons emphasized for using apatite as a support for heterogeneous catalysts is its natural availability. However, very few authors use natural apatite (NAp), probably because the composition and physico-chemical properties are not well controlled. Most of the research teams work with apatites synthesised following the protocol of Sugiyama *et al.* [41]. Regarding NAp, Shaabani *et al.* have used cow bones (**Table 1**, entries 2 and 3) [32, 33]. The latter were combined, for example, with 15 wt.% of manganese (IV) oxide

[32] or anionic complexes of cobalt(II) phthalocyanine (0.4 wt.% Co) [33], affording benzaldehyde with yields of 97 and 95% under air in p-xylene using *8.5% mol of Mn and 0.35% mol of Co per BA*, respectively. In both cases, Shaabani *et al.* introduced non-negligible amounts of base (K_2CO_3 or KOH were added with up to 50% mol *vs.* the alcohol) which makes these systems not very attractive from a Green Chemistry point of view. Indeed, as in many cases in the aerobic oxidation of alcohols, bases are promoting the deprotonation of the alcohol and thus the anchoring of the derived alkoxide to the metal in order to allow its subsequent activation. In addition to the catalyst recycling proved by repeated runs, the use of supports such as apatite would avoid the deactivation of the cobalt complexes (**Table 1**, entry 3) which are prone to yield non-active μ-oxo dimers. It has to be pointed out here that this is not specific to the apatite material. In the case of MnO_2/NAp (**Table 1**, entry 2), the idea was to increase the area to volume ratio of MnO_2 which is detrimental for the bulk oxide. It should be noted that in these studies, little information is given on the anchoring mode of the active phases on the apatite. Apparently, detailed studies of those catalytic materials were difficult to carry out due to the use of NAp. In the case of cobalt phthalocyanine, the authors only mention the advantage of working with a ligand with anionic functions to enhance the deposition of cobalt on the support.

The literature in the field of aerobic oxidation of alcohols includes many more papers dealing with combinations of apatite with either Ru(III) salts (**Table 1**, entries 1 and 4-7) or Pd(II) salts or complexes (**Table 1**, entries 8-9). Like in the previous examples (**Table 1**, entries 2 and 3), the resulting heterogeneous catalysts are generally efficient at temperatures between 60 and 100°C and under atmospheric pressure of pure oxygen or air.

Table 1: Aerobic oxidation of benzyl alcohol (BA) with apatite-based catalysts. Some data have been recalculated from those provided by the authors and are thus reported in italics.

Entry	Support	Loading	Preparation method	Conditions	Yield	Ref
1	Stoich. HA	17.1 wt.% Ru *1.7 mmol.g^{-1}*	I.E. with aq Ru^{III} / 24 h drying 110°C O.N.	Atm O_2 / 80°C / 100 mg cat.mmol ROH^{-1} / toluene / *17 mol% cat*	> 99% Conv. 98-95% Ald (3 h) TOF = 2 h^{-1}	[31]
2	NHA from cow bone	15 wt.% MnO_2 *1.7 mmol.g^{-1}*	$KMnO_4$ 74 h RT + washing + drying 100°C	Air / 80°C / 50 mg cat.mmol ROH^{-1} / p-xylene /8.5 mol% cat + 50 mol% K_2CO_3	97% Ald (3 h)	[32]
3		0.4 wt.% Co *0.07 mmol.g^{-1}*	CoTSPc 48 h RT + washing + drying 70°C O.N.	Air flow/ 100°C / 50 mg cat.mmol ROH^{-1} / p-xylene /0.35 mol% cat + 50 mol% KOH	95% Ald (4 h) TOF = 69.8 h^{-1}	[33]
4	HA calcined at 500°C + aq. $CoCl_2$ 20 min + Wash. Treat.	*c.a. 0.35 mmol.g^{-1}*	aq Ru^{III} / 24 h drying 80°C vacuum 8 h	Atm O_2 / 60°C / 60 mg cat.mmol ROH^{-1} ? / toluene / *2.1 mol% cat*	- (kinetic study at low conv.)	[34]
5	Stoich. HA calcined at 500°C + $CoCl_2$ 20 min or Pb^{2+}, + Wash. Treat.	0.4 mmol.g^{-1}	aq Ru^{III} / 10 min or 24 h drying 80°C vacuum 8 h (also 25, 110 and 180°C)	Atm O_2 / 90°C / 50 mg cat.mmol ROH^{-1} ? / toluene / *1.7 mol% cat*	> 99% Ald (0.75 h) TOF 78 h^{-1}	[35]
6	Method I - Stoich. HA modified by Hacid or Phos (drying vaccum RT, 24 h) Method II - HA synthesized in the presence of prolinol, proline or benzoic acid (drying O.N. 90°C)	0.28 mmol.g^{-1} (0.37 w/o modif) 0.31-0.35 mmol.g^{-1}	aq Ru^{III} / 10 min drying RT vacuum 6 h	Atm O_2 / 60°C / 60 mg cat.mmol ROH^{-1} / toluene / *1.7 to 2.2 mol% cat*	> 99% Ald (0.7-2.6 h) TOF from 21 to 70 h^{-1} 242 h^{-1}	[36]
7	HA-γ-Fe_2O_3	1 wt.% Ru *0.1 mmol.g^{-1}*	aq Ru^{III} RT / 24 h dyring vacuum O.N.	1 bar O_2 flow / 90°C / 50 mg cat.mmol ROH^{-1} / toluene / 0.5 mol% cat	> 99% Conv. 98% Ald (1 h) TOF = 196 h^{-1}	[37]
8	Stoich. HA	0.02 mmol g^{-1}	Impregnation with $PdCl_2(PhCN)_2$ in acetone	O_2 / 90°C / 100 mg cat.mmol ROH^{-1} / trifluorotoluene / 0.2 mol% cat	99% Ald (1 h) *TOF = 495 h^{-1}*	[38, 39]
9	HA	1.1 mmol.g^{-1}	Impregnation with $Pd(OAc)_2$ 3 h + N_2H_4 + washing at reflux	Atm Air / 100°C / 100 mg cat.mmol ROH^{-1} / water / 0.11 mol% cat	95% Ald (7 h) TOF = *123 h^{-1}*	[40]

Ald (Aldehyde); Wash. Treat. (Washing treatment); Stoich (Stoichiometric); I.E. (Ion exchange); O.N. (Overnight)

The use of Ru(III) or Pd(II) precursors combined with apatite allows working without further addition of a base, which is a particularly-attractive advantage in the context of green chemistry. Utilization of apatite in that context was initiated by Kaneda's group [31]. Baiker's group also deeply studied catalysts based on apatite and Ru(III) (**Table 1**, entries 4-6) [34-36]. It is not surprising to find these two metals combined with apatite. Indeed, they are often associated with more classical inorganic supports such as zeolites, alumina, hydrotalcite or carbon [37-40]. Solids like hydroxyapatite, montmorillonite, and hydrotalcite [42] would allow controlling the location of catalytically-active metal species (either in the crystal lattice, or on the surface, or in the interlayer space, respectively), to create of well-defined active metal sites on the solid surface or understand the molecular basis of heterogeneous catalysis.

In the following, we will describe in detail the studies involving Ru(III) and Pd(II), trying to highlight the impact of apatite on the catalytic activity when it is possible to make comparisons. These can only be made a priori if the methods of deposition and activation of the active phases and the catalysis conditions of the resulting catalysts are similar. Finally, it should be noted that, surprisingly, gold hydroxyapatite based systems have not been explored yet for alcohol oxidation reactions, although gold has been used extensively elsewhere in combination with other supports [43].

2.2 Apatite / Ru(III) catalysts

In 2000, Yamaguchi *et al.* reported the first application of apatite-based catalysts using a Ru(III) precursor as the active phase in the partial oxidation of alcohols in liquid phase, with molecular oxygen as an oxidant [31, 44]. According to these authors, the 17 wt.% Ru-HA catalyst was prepared following an ion-exchange (I.E.) procedure involving stoichiometric hydroxyapatite (HA characterized by a molar Ca/P ratio of 1.67) and an aqueous $RuCl_3$ solution for an extended period of 24 h (**Table 1**, entry 1). The resulting material, dried overnight at 110°C, was also characterized by a (Ru+Ca)/P of 1.67, thus validating the exchange of Ca^{2+} by $Ru(III)X^{2+}$ species. EXAFS data confirmed the presence of oxygen atoms in the coordination sphere of Ru^{3+} as well as of one chloro ligand (X = Cl). As a result, the authors considered that the active sites of those catalysts are probably monomeric $RuCl^{2+}$ cations surrounded by O atoms of the phosphate matrix. Aromatic (including heterocyclic ones), allylic as well as aliphatic primary alcohols such as 1-octanol were tested as substrates at 80°C in toluene under 1 atm of O_2 with *17 mol% of Ru per substrate*. In those conditions, very good yields of aldehydes were obtained with the activated alcohols. The oxidation of 1-octanol was the slowest one. Interestingly, nor carboxylic acids, neither their esters (through their reaction with the

starting alcohol) was observed. In the case of BA, three recycling experiments were conducted successfully. From the test of different benzyl alcohols varying by the substitution of the aromatic ring, the authors could establish that the value of the Hammet slope is negative. According to the authors, its value equal to -0.43 is in fact very close to that obtained in homogeneous catalysis with $RuCl_2(PPh_3)_3$ (7) thus validating, monomeric forms of Ru. Similarly, the selectivities (especially primary > secondary alcohols, *e.g.* 1,7-octanediol was chemo-selectively oxidized to 7-hydroxyoctanal in 80% yield) reached in the presence of Ru-HA turned out to be much closer to that of $RuCl_2(PPh_3)_3$ than those of other heterogeneous catalysts such as RuO_2 or Ru/Al_2O_3 [45]. From this result, the authors suggested that, as for $RuCl_2(PPh_3)_3$, the alcohol oxidation would be initiated by the formation of a Ru-alcoholate species and that the carbonyl compound would result from β-hydride elimination in the rate-determining step as evidenced by the strong Kinetic Isotope Effect ($k_H/k_D = 7$) evaluated in the competitive oxidation of BA and its deuterated form. A homolytic mechanism was excluded. Ru-HA catalyst does not involve oxo-ruthenium species as the active oxidant. In the last step of the catalytic cycle (**Figure 1a**), the Ru-hydride species produced with the aldehyde would be converted into a Ru(III)-OOH species by molecular oxygen, that would release H_2O_2 or its decomposition products (H_2O and O_2). According to Kaneda *et coll,* [46] apatite would behave as an inorganic ligand that is robust and tolerant of severe reaction conditions: *e.g.*, strongly oxidizing or reducing environments at high temperatures.

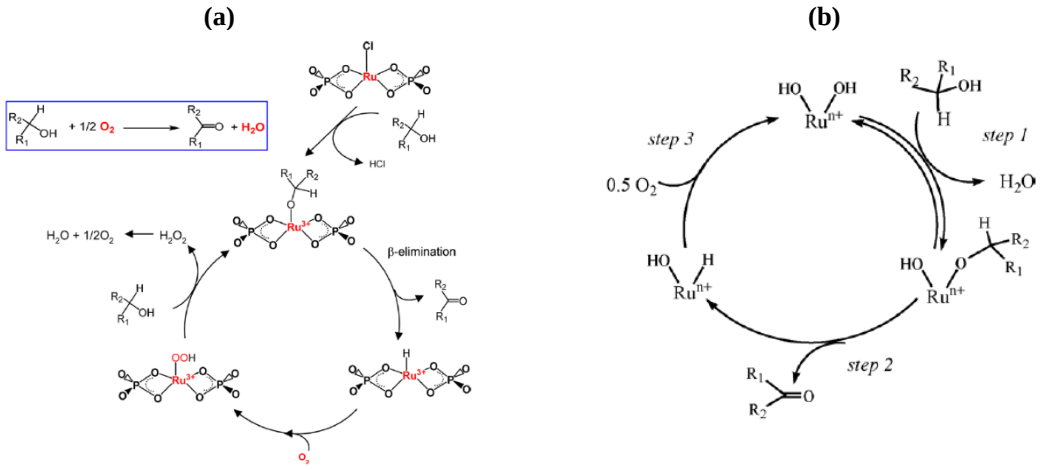

Figure 1. (a) Plausible mechanism of Ru-HA-catalyzed alcohol oxidation. Source: [46]. Adapted with permission of American Chemical Society; and (b) Proposed reaction mechanism for alcohol oxidation over Ru-CoHA. Source [34]. Adapted with permission of Elsevier.

One important drawback of this system is the very low TOF value measured (2 h^{-1}) by the authors because of the high metal content and the relatively large amount of catalyst used. Opre *et al.* re-investigated this type of catalyst in order to better control its structure and thus optimize its performance [34-36]. The first observation made by these authors was that it is not useful to substitute Ca located in the most internal sites by Ru because the latter cannot be accessible to the substrates. Hence, TOF value obtained by the Yamaguchi's group in the case of BA is probably higher than 2 h^{-1}. Opre *et al.* [34-36] also paid close attention to the conditions of introduction of the Ru(III) species. They were particularly concerned about the mechanism of the metal introduction in Yamaguchi's original work. Was it just adsorption to the surface? Was it ion-exchange alone or accompanied by apatite dissolution-precipitation mechanisms or combinations of these processes, in particular in the presence of acidic aqueous solutions such as those of Ru(III)? It is also possible that some restructuration occurs leading, for example, to smaller HA crystallites when long contact times are used? One way to better control these points was to shorten the contact time of the aqueous solution of Ru(III) with apatite from 24 h to 20 min or/and use a modified apatite. Shorter contact time would allow reducing the amount of Ru(III) introduced but also to avoid the dissolution /restructuration of apatite (lot of Ca and P leaching as well as increase of the pH of the contacted solution). Indeed, for longer contact times, Opre *et al.* [35] showed that the Ca+Ru/P molar ratio decreased but this was not the case in the work reported by Yamagachi *et al.* [31]. Opre *et al.* [34-36] also worked to minimize the dehydration of the support by softening the drying conditions of the material recovered after Ru(III) incorporation. They were able to establish that the higher the drying temperature, the lower the activity. Two types of approaches based on modified apatites have been implemented. The first consisted in using apatite previously substituted with divalent cations such as Co^{2+} (**Table 1**, entries 4 and 5) and Pb^{2+} [35], the second being based on the use of apatites synthesized in the presence of polar organic molecules (**Table 1**, entry 6), one of the aims of which is to reduce the size of the crystals formed and thus increase the specific surface area.

Using Co-HA as a support [34, 35] contacted with aqueous Ru(III) solution during 10 min followed by drying under vacuum at 80°C for 8 h afforded catalysts exhibiting TOF values up to 78 h^{-1} in the conversion of BA to benzaldehyde under 1 atm of O_2 at 60°C in toluene (**Table 1**, entry 4, *1.7 mol% of Ru per BA*). It is not clear yet if such improvement of the TOF value for Ru-CoHA is related to an optimized location of Ru on the surface (as shown by a higher Ru/Ca determined by XPS compared to the bulk analysis) or/and to indirect electronic effects of Co^{2+} (it was shown that the incorporation of Co increased the reducibility of Ru for

samples prepared at short times). According to XANES and EXAFS, Ru would be highly dispersed. Simple replacement of Ca^{2+} was excluded and similar structures were established for promoted and un-promoted materials. A point of divergence between the groups of K. Kaneda and A. Baiker also concerned the presence of a chloro ligand in the coordination sphere of ruthenium once the latter was incorporated into the apatite. Clearly, no Cl^- could be detected by XPS and the occurrence of a $Ru(OH)_2^+$ species (**Figure 2**) with the reaction mechanism of **Figure 1b** was preferred in the work of Opre *et al.* [34]. The catalytic activity in alcohol oxidation was partially lost by drying the catalyst at temperatures above 80°C, presumably, due to irreversible dehydration of the active species.

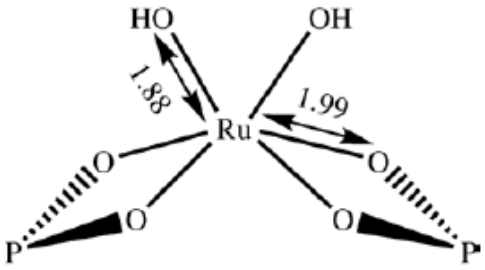

Figure 2. Proposed structure of the Ru species in Ru-CoHA. Source:[34]. Adapted with permission of Elsevier.

Excellent yields of aldehydes with reasonable TOF values (> 20 h^{-1}) were also obtained with substituted BA as well as heterocyclic alcohols. The oxidation of allylic alcohols was also complete but at a slower rate. Octanol-1 oxidation was reasonably fast without octanoic acid formation at short reaction times (less than 1 h) but it can be noticed that, for longer reaction times, the formation of the carboxylic acid could not be avoided, maybe as the result of the oxidation of some Co^{2+} into Co^{3+}. Like for simple Ru-HA, competitive reactions between primary and secondary alcohols showed that the primary alcohols are more reactive. Interestingly, these authors performed a "hot filtration" test as recommended by Sheldon [47]. No further reaction occurred when the solid was removed after 40% BA conversion. *In situ* EXAFS study of the Ru-CoHA catalyst (Co-HA with $RuCl_3$ for 24 h) during BA oxidation emphasized that no reduction of Ru^{3+} in Ru^0 occurs and agreed with the possible formation of Ruthenium alcoholate species. Carrying out the reaction at 40°C under argon, the conversion of BA stopped at 4.7% after 10 min meaning that the reaction obeys a kind of Mars and Van Krevelen mechanism [28, 48]. In the absence of O_2, the active sites are "reduced" during the reaction and thus become inactive for further reaction. Moreover, considering the amount of catalyst (Ru) used in these conditions, the authors concluded that half of the Ru sites would be accessible.

The other approach initiated by Opre *et al.* consisted in using apatites with surfaces modified by the introduction of water-soluble polar organic molecules [36, 49] (alkyl phosphates, alkenoic acids or amino-acids) able to form strong hydrogen bonds with the OH and phosphate functions of hydroxyapatite (**Table 1**, entry 6). These molecules were used either during (case of proline, prolinol, benzoic acid (BAcid), drying at 90°C) or after (case of hexanoic acid (HAcid) or 2-ethylhexylphopshate (Phos), drying 24 h/RT) the synthesis of the hydroxyapatite support. Ru was later introduced at room temperature and for short contact time followed by a filtration step. Materials prepared by incorporation of the molecules in the synthesis gel afforded catalysts with the best TOF values. Considering the oxidation of BA at 60°C under 1 bar O_2 in mesitylene, instead of toluene, Ru-HA-BAcid was characterized by a TOF of 242 h^{-1} at 100% conversion (with no further oxidation of benzaldehyde to benzoic acid) which is 3 times better than Ru-CoHA [28] and more than two order of magnitude than Ru-HA [31]. Again, Ru-HA turned out to be a good and highly selective catalyst for aromatic and allylic alcohol but sluggish transformations were obtained with aliphatic primary and secondary alcohols. The authors think that higher intrinsic activity of Ru related to some modification of its coordination sphere is a more plausible explanation of the good catalytic performances of the resulting materials than the increase of the accessible active sites. Indeed, based on DRIFT, SEM, STEM-EDX, ICP-OES, and BET measurements, it could be concluded that the location and coordination of Ru is different in organically modified HA. Upon the introduction of Ru, no exchange of Ca^{2+} could be observed. In the resulting materials, the incorporation of Ru would not result from an ion-exchange process but from an adsorption process controlled by the polar organic molecules. It has to be noticed that, according to the authors, those modifiers are removed during Ru incorporation (washing and drying at room temperature for 6 h). The method using prolinol, proline or benzoic acid in the synthesis gel of hydroxyapatite led systematically to non-stoichiometric materials and also to a reduced crystallite size giving rise to better specific surface areas.

Regarding kinetic studies, Opre *et al.* [34-36] have underlined the importance of operating conditions where there are no mass transport limitations. In these reactions, the removal of water from the surface of the catalysts is slow and can be rate-limiting. That is the reason why, non-volatile solvents are used at temperatures close to their boiling point in order to favor the elimination of water. However, if those solvents are used at temperatures too close to their boiling point, there is a risk of decreasing the oxygen partial pressure making the re-oxidation step of Ru rate-limiting instead of the β-elimination. Using solvents with very high

boiling point in lesser amounts or less catalyst is recommended. Those authors confirmed that under truly kinetically controlled conditions, electron withdrawing substituents of benzyl alcohol have a decelerating effect [36] thus agreeing with a rate-limiting β-hydride elimination step (**Figure 3**). This was exactly the opposite in the case of cobalt phthalocyanine/apatite [33] where an autoxidation mechanism was proposed by Shaabani *et al.* In the work of Opre *et al.* [34], the K.I.E. value measured at 5% BA conversion in the case of Ru-CoHA was equal to 1.6 under kinetically controlled conditions and only 1.2 under transport limited conditions which is rather small but also agrees with β-hydride elimination as the rate determining step. According to these authors, re-oxidation of the ruthenium site should definitely not limit the overall reaction rate in the oxidation of aliphatic alcohols which are less reactive than BA.

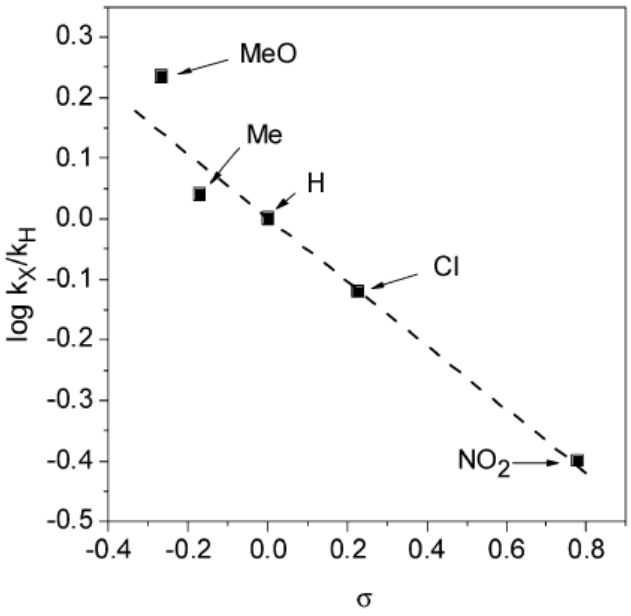

Figure 3. Hammet plot of *p*-substituted benzyl alcohols oxidation. Reaction conditions: 1 mmol *p*-X-benzylalcohol (X = H, Cl, NO_2, Me or MeO), 10 mg RuHA-BAcid (0.0031 mmol Ru), 4 mL mesitylene, 60°C, 1 bar O_2, t = 2 min. Source: [36]. Adapted with permission of Elsevier.

Later, Mori *et al.* used HA-γ-Fe_2O_3 materials made of magnetic γ-Fe_2O_3 nanocrystallites dispersed in a hydroxyapatite matrix instead of HA as a support for Ru-based oxidation catalysts (**Table 1**, entry 7) [37]. After Ru^{3+} introduction at a much lower loading than in their initial work (1 wt.% instead of 17) using an impregnation at room temperature, they showed that highly dispersed monomeric Ru species could be obtained. These prepared catalysts afforded a significant improvement in activity in comparison with Ru-HA [31] with very interesting separation properties with an external permanent magnet, thus facilitating recycling experiments. One of the reasons was the increase of the BET surface area (115 m^2/g instead of

49 m^2/g for conventional Ru-HA) that would result from the suppression of the crystal growth. In this work, involving EXAFS measurements also, the authors agreed with Opre *et al.* and proposed the occurrence of $Ru(OH)_2^+$ with six coordinated oxygen atoms (two from hydroxo and four from phosphato ligands). By analogy with the use of Co-HA [34, 35], HA-γ-Fe_2O_3 would promote some electron transfer from Ru(III) to Fe(III) affording Ru(IV) oxidizing species. Catalysis tests with benzylic (or heterocyclic), allylic and aliphatic primary alcohols as well as with primary alcohols with cyclopropyl substituents at 90°C under O_2 flow in toluene with *0.5 or 1 mol% of Ru per substrate* showed that the double bonds or the cyclopropyl rings are not touched. In contrast to the systems described before, Ru/ HA-γ-Fe_2O_3 led to the aerobic oxidation of aliphatic alcohols (*e.g.* 1-dodecanol) into their corresponding carboxylic acids. According to the authors, those catalysts were as efficient with sterically hindered substrates as their soluble analogs (homogeneous catalysis), thus emphasizing the location of most of Ru sites on the external surface of the apatite crystals. Secondary alcohols could be converted almost completely into ketones in the same conditions, especially when using 5 atm of O_2. The authors have claimed TOF values of 196 h^{-1} for BA instead of 2 h^{-1} in their original work (17wt.%Ru/HA [31]) and 78 h^{-1} for Ru-CoHA described by Opre *et al*. [34, 35]. The addition of radical traps or clocks led to the conclusion that no radical intermediates would be involved. Apparently, some oxidation tests with BA could be performed even at room temperature for 24 h but the amount of catalyst used in these examples was quite important. However, it can be noticed that other groups describing tests in so mild conditions in the literature proceeded with the addition of a base [50-52]. No structural changes upon the catalysis test could be detected.

2.3. Apatite / Pd(0) catalysts

Palladium is also a transition metal widely used in aerobic oxidation catalysis [53, 54]. Heterogeneous catalysts based on Pd(0) and supports like activated carbon, pumice, hydrotalcite, oxides, or even organic polymers have been reported [55]. Usually, those materials suffer from low catalytic activities and a limited substrate scope. In the case of primary alcohols, the selectivity in aldehyde is rather low. Support effects on alcohol conversion and product selectivity have been mentioned many times [1]. Carbonaceous supports are notorious for their gas adsorption capacity which may have some impact on the catalytic performance. Alumina with fairly large specific surface areas are known for their ability to disperse Pd and to stabilize single-site Pd^{2+} catalytic centers but selectivity and conversion values are rather low. Optimum Pd(0) particle sizes have been reported for benzyl alcohol oxidation which implies that such

reaction is structure sensitive, with edge and corner Pd atoms more active than terrace sites [56].

In 2002, Kaneda *et al.*, reported a pioneering work on the use of apatite for the development of supported Pd catalysts that turned out to be very successful, among the best, in the selective oxidation of alcohols using O_2 at atmospheric pressure (**Table 1**, entry 8) [38, 39]. Other supports such Al_2O_3, SiO_2 and C are known to lead to less aldehyde and more acid. In this study, the authors investigated the influence of the stoichiometry of the apatite support, working either with HA-0 (stoichiometric apatite, $Ca_{10}(PO_4)_6X_2$, where X is a monovalent anion such as OH^-, F^-, or Cl^-) or HA-1 (non-stoichiometric, calcium-deficient HA, $Ca_{10-n}(HPO_4)_n(PO_4)_{6-n}(OH)_{2-n}$ (n = Ca^{2+} vacancies) with Ca/P ratio <1.67). Both types of materials were impregnated by an acetone solution of $PdCl_2(CH_3CN)_2$ leading to two kinds of bound Pd complexes with similar low Pd loadings (0.02 mmol g^{-1}) despite the presence of up to 0.42 mmol g^{-1} of PO_4^{3-} on the apatite surface. Thereafter, monomeric Pd(II) species could be pointed out in both cases but Pd to Cl was 1:2 for PdHA-0 and chlorine was not detected in the case of PdHA-1 leading to the proposals shown in **Figure 4**.

Figure 4. Proposed surface structures around Pd(II) center of (a) PdHA-0 and (b) PdHA-1. Source: [38]. Adapted with permission of American Chemical Society.

PdHA-0 gave rise to a very efficient catalyst in the aerobic oxidation of BA while PdHA-1 did not. Almost complete conversion of BA into benzaldehyde was reached in 1 h with *0.2% mol of Pd per BA* at 90°C under 1 atm of O_2 in trifluorotoluene (**Table 1,** entry 8). Oxidation of a wide variety of other benzylic and allylic alcohols giving the corresponding ketones and aldehydes was reported in the same conditions. Aliphatic and heterocyclic alcohols needed more Pd catalyst (*0.6% mol Pd per substrate*) to reach completion. With BA and 1-phenylethanol, oxidation tests could be even performed in water with only *0.04% mol Pd per BA* but at 110°C. Last but not least, a large-scale reaction was carried out with pure 1-phenyl ethanol at 160°C during 24 h with 4×10^{-4} *% mol Pd per mol of substrate* giving rise to a TON of 236 000 (TOF of 9800 h^{-1}) [39]. The lack of activity of PdHA-1 might be explained by the coordination of heteroatoms to the Pd(II) centers, thus preventing their reduction to Pd(0).

According to the authors, the behavior of Pd-HA0 was analogous to that of Pd nanoclusters such as $Pd_{561}phen_{60}$-$(OAc)_{180}$ and $Pd_{2060}(NO_3)_{360}(OAc)_{360}O_{80}$. Hence, Pd(II) would be converted *in situ* into Pd(0) during alcohol oxidation as demonstrated by the presence of an induction period in the time profile for PdHA-catalyzed oxidation of 1-phenylethanol at 90°C in trifluorotoluene under O_2 atmosphere. This was confirmed by TEM (average diameter of 3.5 nm) and Pd K-edge XAFs analyses. Using normalized TOF values, the authors suggested that the oxidation of the alcohols would occur at the low-coordination sites of the nanoparticles.

One mechanism that is generally proposed for $Pd(II)X_2$ catalyzed aerobic oxidation of alcohols is based on the formation of a Pd(II) alcoholate intermediate assisted by the deprotonation of the alcohol in the presence of an exogenous base, B, leading to the formation of BH^+X^-. Then, a Pd(II) hydride intermediate is formed upon a β-hydride elimination mechanism that is followed by a reductive elimination on the Pd(II)HX complex affording Pd(0) and HX. Pd(0) is finally re-oxidized to Pd(II) and the two X ligands reintegrated in the coordination sphere of Pd as shown in **Figure 5 a**. Here, no additional base is required. The authors propose instead the occurrence of an oxidative addition step of the O-H bond of the alcohol to coordinately unsaturated Pd(0) atoms at the edge of the nanoparticles. Those Pd(0) atoms would be regenerated in two steps. First, a β-elimination would afford the carbonyl compound and a dihydride Pd(II) intermediate, then the latter would react with O_2 leading to H_2O_2 (or H_2O + ½ O_2) and Pd(0) (**Figure 5 b**).

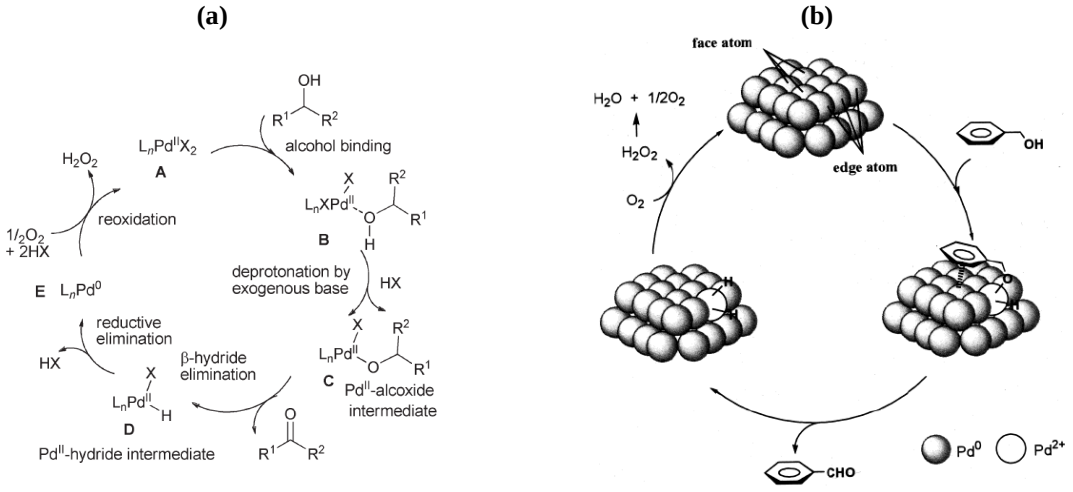

Figure 5: (a) Generally accepted mechanism of the aerobic Pd(II)-catalyzed oxidation of alcohols. Source: [1]. Adapted with permission of RSC; and (b) Possible reaction mechanism for the oxidation of alcohols on the surface of Pd nanocluster. Source:[39]. Adapted with permission of American Chemical Society.

Aerobic oxidation of benzyl alcohols in water was also reported by Paul *et coll.* [40]. Those authors proceeded by the impregnation of HA with a Pd(II) complex, *i.e.* $Pd(OAc)_2$, but unlike Kaneda *et coll*, a reducing agent, *i.e.* hydrazine, was used to obtain Pd(0) nanoparticles of 20 nm average diameter (**Table 1**, entry 9). Excess of $Pd(OAc)_2$ was removed prior to the catalysis tests. It should be noted that this catalyst was much less efficient than the one reported by Kaneda *et coll*. Indeed, Paul *et coll.* had to introduce *c.a.* 50 times more Pd (*0.11 mol% vs. 0.02 mol% of Pd per substrate*) for the oxidation of BA in order to obtain a 95% yield of benzaldehyde in 7 h at 100°C instead of 1 h in the work of Kaneda *et al*. [38-39]. This strong difference in reactivity may be related to the use of air instead of O_2. It is also likely that the size of the nanoparticles is too large. The oxidation of an aliphatic primary alcohol (1-pentanol), not described in the work of Kaneda *et coll.* [38-39], showed that the reaction was much difficult (72% yield after 48 h) but, importantly, pentanal was shown to be selectively formed (no pentanoic acid). The absence of added base with apatite supported Pd(0) catalysts would be responsible for such selectivity in aldehydes in water [40]. Indeed, the oxidation of aldehydes to acids is known to be favored in alkaline water because aldehydes undergo hydration to gem diols that are easily transformed into carboxylic acids.

3. Gas phase reactions

3.1. Partial oxidation of methane

Methane is an important alternative for the replacement and the diversification of the conventional sources of energy. Hydroxyapatite-based catalysts have been investigated for its various valorisation routes through oxidative coupling, steam or dry reforming or partial oxidation of methane (POM) [2, 41, 57-64]. Only the studies related to the POM reaction ($CH_4 + 1/2\ O_2 \rightarrow CO + 2\ H_2$) will be considered in this chapter that is devoted to the selective oxidation in the presence of oxygen. Steam reforming of methane (SRM) is the dominant commercial process and is of interest for hydrogen for fuel cells applications since it provides H_2/CO ratio ≥ 3. However, compared to POM of methane, SRM exhibits some drawbacks: it is highly endothermic, it is operated under high pressure and CO_2 is significantly produced by water-gas shift reaction. POM is comparatively more energy efficient since mildly exothermic and may be suitable for Fischer-Tropsch synthesis which requires H_2/CO ratio close to 2 [2, 65].

Supported zerovalent Ni and Rh, are accepted to be active catalysts for POM. Rhodium is known as the most active for POM, but Ni was the most extensively studied metal because it is effective and cheaper [66]. The related supported catalyst studies emphasized that strategies to avoid sintering and coke formation should to be developed [66, 67], and suggested that high dispersion of metal species and/or use of alkaline earth metals may be beneficial to improve the catalytic performance for the POM.

In this context, the Ni strontium hydroxyapatite system has been first investigated by Yoon *et al.* [65, 68, 69]. SrNiA(a) catalysts (with a = 100 × Ni/(Sr+Ni) molar percentage varying from 1 to 20%) were prepared by a coprecipitation preparation route but, from XRD, mixtures of nickel substituted strontium hydroxyapatite and of strontium phosphate ($Sr_3(PO_4)_2$) were rather obtained. Their relative proportions were reported to depend on the Ni content and the final global (Sr+Ni)/P molar ratios were found to vary in a large extent, from 1.5 to 3. Although metallic Ni was not detected on the calcined samples, no pre-reduction was required to get excellent catalytic performance. Ni addition significantly improved the results compared to Ni free HA, and at 800°C, with $P(CH_4)/P(O_2)= 2$ and $W/F= 10$ mg min^{-1} mL^{-1} (W and F being the catalyst weight and the total gas flow rate, respectively). The best CO and H_2 yields were achieved for Ni/(Sr+Ni) molar ratio of 0.15, with excellent H_2 yield of 90 % which is even slightly above the equilibrium, probably due to the existence of hot spots. They observed a hysteresis upon sequential increase and decrease of the reaction temperature (**Figure 6**) and proposed that the catalyst was activated under the reducing reaction environment. This was ascribed to the extraction of Ni out of the phosphate matrix that generates highly dispersed Ni metallic active species under the reactional reductive conditions.

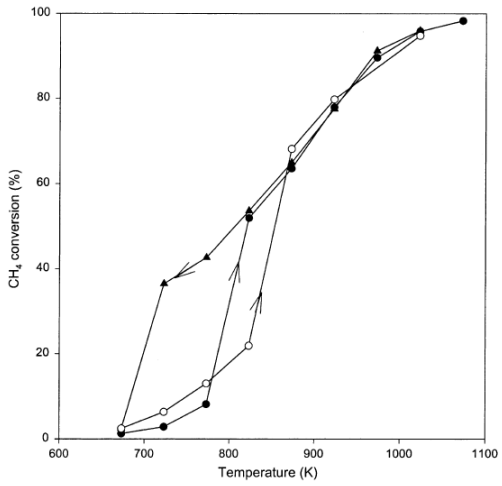

Figure 6: Methane conversion with sequential temperature increase and decrease over SrNiA(10), (●) first increase, (▲) decrease, (○) second increase. Source: [68]. Adapted with permission of Elsevier.

Nickel calcium hydroxyapatite system was further investigated [65]. Coprecipitation was carried out at high pH, but varying the Ca/P and Ni/P precursor molar ratios in a quite large range. In these conditions, the authors obtained mixtures of calcium phosphate, calcium hydroxyapatite, calcium nickel phosphate, calcium nickel hydroxyapatite and NiO (for high Ni loadings) (**Figure 7A**). Measuring the performance at lower contact time ($P(CH_4)/P(O_2) = 2$, W/F= 2 mg $min^{-1}mL^{-1}$) than in their former study dealing with the strontium hydroxyapatite [68], they reported excellent performance. At 800°C, the methane conversion reached 93%, with CO and H_2 selectivities of 96 and 90%, respectively [65]. They once more concluded to the extraction of nickel out of the matrix during the POM reaction. Following the system upon sequential increase and decrease of the reaction temperature (see **Figure 6**) with related TPR, TEM, EDS, XPS characterizations, they described the evolution for the catalyst (**Figure 7**). They reported that the conversion abruptly rose from a given reaction temperature, which is explained by the reduction of NiO by the produced H_2 and CO (**Figure 7B**). In addition, in these operating conditions, the nickel present in the phosphate or apatite structures gradually got out of the phosphate matrices, formed fine particles and was reduced (**Figure 7B**). It was inferred that most of the catalytic activity should be attributed to such highly dispersed metal particles. Upon decreasing the reaction temperature, gradual reoxidation occurred, resulting in the formation of a thin layer of NiO layer onto the surface metallic nickel entities, while the extracted nickel did not go back to the phosphate or the apatite structure (**Figure 7C**). The metal state and high catalytic performance could finally be recovered upon simple increase of the reaction temperature to 450°C (**Figure 7B**). Compared to the other Ni catalysts, Ni from calcium phosphate/hydroxyapatite catalysts was found to be more easily reduced, which may explain the peculiar ability of this system to be activated under reaction feed at a relatively low temperature (at or below 650°C).

The reaction mechanism over this system was also investigated thanks to pulse experiments [69]. It was shown that the reaction occurs primarily *via* the direct dissociation of methane. In addition, while metallic nickel was accepted to be an essential active component in POM, given that fully reduced catalyst exhibited lower activity, it was suggested that both metallic Ni and partially oxidized nickel might be required to get high activity and selectivity [69].

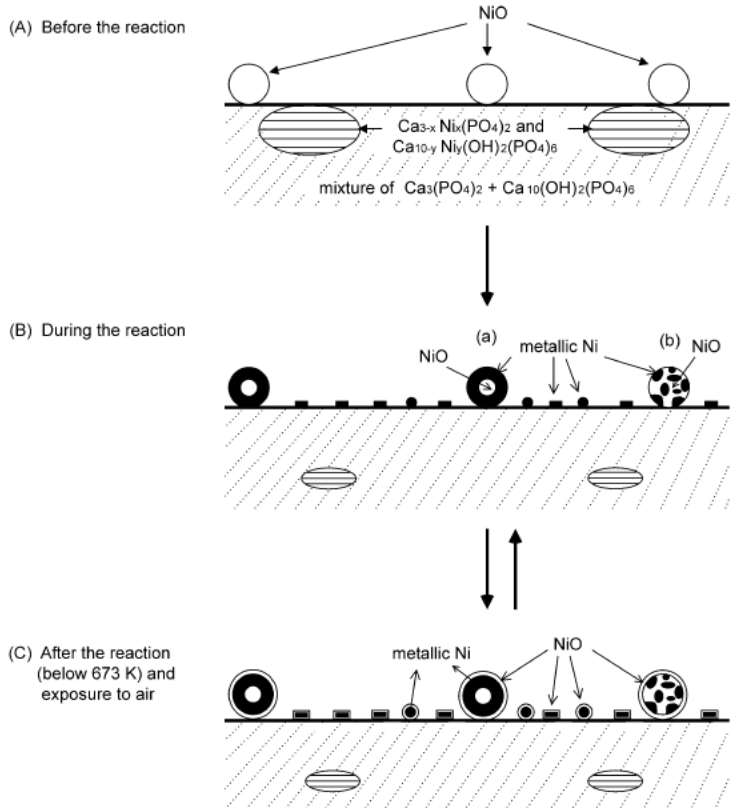

Figure 7: Proposed scheme of changes of Ni state in POM reaction. Source: [65]. Adapted with permission of Elsevier.

A different reaction mechanism, a two-step mechanism (complete methane oxidation followed by reforming of the residual methane with the primarily produced CO_2 and H_2O) was assumed by Boukha *et al.* who investigated rhodium impregnated onto non-stoichiometric hydroxyapatite (Ca/P= 1.5). Various Rh weight loadings (x = 0.5, 1 and 2 wt%) have been considered (Rh(x)/HA catalysts). From XRD, TEM, TPR, XPS and DRS (Diffuse reflectance spectroscopy) characterizations, it was found that Rh existed in three different forms in the samples as: (i) large crystallites of Rh_2O_3 deposited on the surface, (ii) RhO_x in small particles exhibiting strong interaction with the support and (iii) Rh^{2+} species incorporated in the calcium vacancy site of the hydroxyapatite. Upon reduction at high temperature, the appearance of a new diffraction line ascribed to calcium triphosphate (TCP) showed that the incorporated Rh favors the thermal transformation of HA to TCP, which may be responsible for the decrease of specific surface areas observed as Rh loading increases. The POM reaction was carried out over the Rh(x)/HA catalysts after *in situ* reduction at 727°C in the following conditions: $P(CH_4)/P(O_2) = 2$, W/F = 0.3125 mg min^{-1} mL^{-1}. Comparison of the three Rh catalysts pointed out the structure sensitivity of the Rh particles spread over the HA carrier. The best

performances were obtained for Rh(1)/HA, where methane conversion, 53% at 600°C, exceeds 46%, obtained for Rh/SiO_2 in similar operating conditions. In addition, the H_2/CO ratio was always higher than 2, and the value obtained at 700°C (2.1) appears suitable for Fisher Tropsch downstream application. The conversion and products yields were found to be very stable at least for 30 h at 700°C (76% conversion for Rh(1)/HA) which was explained by excellent resistance against coking. Note that, despite the limited specific surface area of its carrier (here 33 m^2g^{-1} in the synthesis conditions applied) that was detrimental to the dispersion of rhodium, this catalyst was also found excellent for the SRM reaction. The best performance obtained for the Rh(1)/HA composition for the two reactions was explained by its higher thermal stability ascribed to its lower fraction of incorporated Rh^{2+} species that hindered its thermal transformation into TCP.

3.2. Alkane oxidative dehydrogenation reactions

In the context of the increasing gap between the production and the demand in olefins on the world market, especially in the cases of ethylene and propylene, their production from corresponding alkanes is of great interest [4, 8, 11, 70-73]. Up to now, commercial productions of alkenes from alkanes were carried out in the absence of oxygen. However, the dehydrogenation reactions suffer from high endothermicity and thermodynamic limitations which can be overcome by operating at high temperature. In these conditions, carbon deposition on the active sites is responsible for deactivation [74]. The introduction of oxygen in the reaction feed appears more appealing since it allows performing exothermic oxidative dehydrogenation reactions (ODH), eliminates thermodynamic limitations and prevents the growth of carbonaceous deposits over the catalysts [11, 75]. However, such alternative ODH routes for the production of olefins ($C_nH_{2n+2} + 1/2\ O_2 \rightarrow C_nH_{2n} + H_2O$) still remain challenging. Yet no catalyst has been found efficient enough to produce competitive ethylene or propylene yields [11, 72].

The main challenge in the gas phase mild oxidation reactions is to achieve the selective activation of the C-H alkane bond at temperature low enough to limit over-oxidation of both the alkane reactant and the alkene targeted product [11, 71]. Although the limiting step of the ODH reactions is commonly believed to be the abstraction of hydrogen from the adsorbed alkane [18, 74, 76, 77], there are still open questions about this activation step [71] and the factors governing the alkene selectivity [11, 78]. The proposed mechanisms for oxidative dehydrogenation of light alkanes over catalyst containing a reducible metal are essentially based on the Mars and Van Krevelen mechanism [48], which involves the cleavage of C-H bond,

participation of lattice oxygen and its *in situ* regeneration by gaseous oxygen present in the feed. Catalysts are therefore based on supported or bulk TMI, but their compositions depend on the nature of the alkane considered. It is well accepted that highly-polymerized oxide-like catalytic species are detrimental to the control of the alkene selectivity, but it is still controversial whether metal units with limited nuclearity (involvement of ensemble effects) or isolated species should be favored [79-82]. In addition, the influence of acid–base properties of the support and of the nature of its interactions with the active phase have been recognized for many years [83]. Acid-base properties impact both conversion and selectivity of ODH reactions [12, 83]. On the one hand, basic properties, although less often studied than acidic ones may play a key role in the activation of the C-H bond. On the other one, according to Grzybowska *et* coll., low acidity and high basicity should favor the desorption of the olefin [77, 84].

In this context, metal modified HA have been considered as potential candidates for the oxidative dehydrogenation of alkanes. HA should not be considered only as a simple carrier to disperse the TMI active phase, since its tunable acid-base properties make it an original co-catalyst. In addition, the numerous opportunities offered by the modulation of its composition by either cationic or anionic metal ions makes it a unique catalyst system. The conditions of metal deposition (coprecipitation, ion-exchange or impregnation as well as metal loading) are thus key parameters impacting the metal dispersion and its surface availability.

3.2.1 Catalytic performance of the metal modified hydroxyapatite in the ODH reactions

Table 2 gathers some results reported in literature for metal modified HA used in the oxidative dehydrogenation reaction of several alkanes. For the sake of comparison, the results are presented for the same reaction temperature for a given alkane, and the operating conditions have been reported using a homogeneous presentation for the reaction parameters. In line with the high demand in propylene, the oxidative dehydrogenation of propane (ODHP) was the most investigated up to now (**Table 2**, entries 1-8). Several metals, vanadium (**Table 2**, entries 1-5), cobalt (**Table 2**, entry 6), chromium (**Table 2**, entry 7) and iron (**Table 2**, entry 8), have been considered. Those metals have been introduced with different loadings using several preparation methods (**Table 2**). One pot coprecipitation synthesis was achieved in the case of vanadium, the metal precursor being introduced in solution with P and Ca (or other alkaline earth metal) (**Table 2**, entries 1, 4, 5) [85, 86]. In these conditions, despite only a very limited fraction of the introduced metal is accessible on the surface, the modification of the bulk apatite could induce some benefit on the surface reactivity [87, 88]. Cation-exchange and wet

impregnation were also commonly achieved for the ODHP reaction. In practice, the protocols are very similar except there is no washing step in the case of impregnation, and this later method also allows reaching higher metal loading. As shown in **Table 2**, in most cases (entries 1,2,5,7-10, 13, 14), the optimal performance was obtained for low or intermediate metal loading, emphasizing that an optimal surface dispersion should be achieved. Although greatly dependent on the synthesis conditions, the highest propylene selectivity was obtained for the vanadium system. The vanadium impregnated system was also used for the oxidative dehydrogenation of *n*-heptane (**Table 2**, entry 12) and *n*-octane (**Table 2**, entries 13, 14) that were taken as models for medium chain length linear paraffins [89-92]. Beside octenes, other mild oxidation products were formed in increasing proportions as the vanadium loading increases. The ODHE reaction was also studied on cobalt modified apatites (**Table 2**, entries 9, 10). Despite the activation of ethane is known to be very challenging due to the very high stability of its C-H bond, promising results were reported for this system that remains stable even for high reaction temperature.

The results obtained for the various metal are detailed in the next section. Common general features observed for the investigated systems will finally allow to discuss how the hydroxyapatite structural properties assist the transition metal in the activation of the alkane.

Table 2: Explored metal modified hydroxyapatite systems (Calcium HA, except otherwise mentioned) and related properties and catalytic performance (alkane conversion and alkene selectivity) reported for the optimal composition in the mentioned conditions and at a fixed reaction temperature T_R for a given alkane. In the case of n-octane, beside selectivity in octenes, the global selectivity in aromatics and mild oxygenated compounds is additionally provided in parentheses. To facilitate the comparison, metal loading M wt%, and operating conditions are reported in a homogeneous way. Some data have been recalculated from those provided by the authors and are thus reported in italics.

*for one pot coprecipitation syntheses the metal loading gathers metal distributed both in the bulk and on the surface.

£ the weight has been varied to compare the system in the same conversion range.

Entry	Alkane (reaction temperature)	Metal	Metal deposition method and the M loading range explored	Composition Properties	M wt%	SSA (m^2g^{-1})	Operating conditions	Conv. (%)	Sel. (%)	Ref
1	**Propane** (T_R = 450°C)	**V**	One pot coprecipitation V/P= 0 →0.15	V/P=0.10 *$Ca_{10}(PO_4)_{5.4}(VO_4)_{0.6}(OH)_2$*	*2.6**	62	*$P(C_3H_8)/P(O_2)$= 3.5* *W/F= 16.7 mg min^{-1} mL^{-1}*	16.5	54.2	[86]
2			Wet impregnation				*$P(C_3H_8)/P(O_2)$= 3.5*			[93]
			0-10 wt%VOx / CaHA		2.5	53	*W/F= 16.7 mg min^{-1} mL^{-1}*	10.8	48.1	
			/ SrHA		5	34		12.7	62.5	
3			wet Impregnation				*$P(C_3H_8)/P(O_2)$= 3.5*			[94]
			0-10 wt% VOx / BaHA		5	12	*W/F= 16.7 mg min^{-1} mL^{-1}*	4.4	26.5	
4			One pot coprecipitation at constant pH = 9 *$Ca_{10}(PO_4)_{6-x}(VO_4)_xOH)_2$ (x 0 →1)*	Ca/(V+P) = 1.66 V/P = 6.69 *$Ca_{10}(PO_4)_{0.78}VO_4)_{5.22}(OH)_{2-yOy}$*	*24**	*20*	*$P(C_3H_8)/P(O_2)$= 3.7* *W/F= 8 mg min^{-1} mL^{-1}*	5	27	[87]
5			One pot coprecipitation with periodic base addition	$Ca_4V_4O_{14}$:V-HA =5:95 wt% Epitaxial growth	*18.7**	28	*$P(C_3H_8)/P(O_2)$= 3.7* *W/F= 8 mg min^{-1} mL^{-1}*	8.5	44	[88]
6		**Co**	Ion exchange from SrHA	Sr/P= 1.53 1000Co/Sr (at)= 55	*2.1*	56.1	*$P(C_3H_8)/P(O_2)$= 3.5* *W/F= 16.7 mg min^{-1} mL*	23	48.6	[95]
7		**Cr**	Ion exchange 0-3.7wt%	(Cr+Ca)/P~ 1.5	~1.5	53-61	*$P(C_3H_8)/P(O_2)$= 2* W/F = 0.66 *mg min^{-1} mL^{-1}*	13	~30%	[5]
8		**Fe**	Ion exchange 0.5-5.4wt%	(Fe+Ca)/P= 1.63	0.5	42	*$P(C_3H_8)/P(O_2)$= 2* W/F= 0.83 *mg min^{-1} mL^{-1}*	~4	~32-35	[96]
9	**Ethane** (T_R = 550°C)	**Co**	Ion exchange 0-1.35wt%		1.1	34-40	*$P(C_2H_6)/P(O_2)$= 2* *W/F adjusted* £	35	60	[10]
10			Wet Impregnation 0-14 wt%		0.96	48-52	*$P(C_2H_6)/P(O_2)$= 2* *W/F adjusted* £	16	53	[97]
11	**Isobutane** (T_R = 450°C)	**Cr**	Wet Impregnation 0-7wt%	Ca/P = 1.67	7	52.5	*$P(iC_4H_{10})/P(O_2)$= 1.17* W/F= 16.67 *mg min^{-1} mL^{-1}*	24.4	31.1	[98]

12	***n*-heptane** (T_R = 500°C)	**V**	Wet impregnation 15wt % / CaHA / SrHA, / MgHA / BaHA	M/P = 1.65-1.63	15	9-12	*P(n-C_7H_{16})/P(O_2)= 2* GHSV = 4000h^{-1}	 23 25 30 26	 42 43.5 39 47	[89]
13	**n-octane** (T_R = 450°C)	**V**	Wet Impregnation 2.5-15 V_2O_5 wt%	Ca/P = 1.51, SS of the support 72 m^2g^{-1} V_2O_5 ≥10wt %, additional pyrovanadate phase	*0.7(2.5)* *3 (10)*	51 13	*[O_2] not provided* GHSV = 4000 h^{-1}	29 22	66 (7) 58 (14)	[90]
14			Wet Impregnation 5 V_2O_5wt % / SrHA 7.5 V_2O_5wt % / SrHA 15 V_2O_5wt % / SrHA	Sr/P = 1.64 SS of the support 81.2 m^2g^{-1} V_2O_5 (+ pyrovanadate for15 wt%)	 *1.45* *2.2* *4.7*	 45.7 38 9.5	*P(n-C_8H_{18})/P(O_2)= 1* GHSV = 4000h^{-1}	 25 30 33	 75 (10) 60 (25) 56 (29)	[99]

3.2.2 Metal ion modifications

3.2.2.1 Modifications by metal cations

Divalent cobalt ions

Several studies emphasized the advantageous role of cobalt in redox catalysis [100-103]. Both cobalt modified calcium (Co-HA) (**Table 2** entry 6) [10, 97] and strontium (Co-SrHA) (**Table 2**, entries 9, 10) [95] hydroxyapatites have been studied for ODHP and ODHE reactions, respectively. Since the influence of the metal loading was investigated for both impregnation and ion exchange deposition methods these Co-apatite systems provide appropriate model systems to discuss the influence of the speciation and dispersion of this redox center, that can be present as isolated centers or polymeric entities.

In the case of Co-SrHA samples obtained by the ion exchange procedure [95], the formation of supported $CoO/Sr_{10}(PO_4)_6(OH)_2$ was discarded by XANES characterization [104]. Based on the unicity of the PO_4 ^{31}P NMR signal, the authors concluded to the formation of $Sr_{10-x}Co_x(PO_4)_6(OH)_2$ rather than a mixture of $Sr_{10}(PO_4)_6(OH)_2$ and $Co_{10}(PO_4)_6(OH)_2$ (**Figure 8A**). They did not precise if this $Sr_{10-x}Co_x(PO_4)_6(OH)_2$ formulation refers to the formation of a bulk solid solution or if the cationic substitution (achieved by ion exchange) is limited to the surface. This is questionable, since, given the acidic pH of the exchange solution, dissolution-precipitation may possibly occur, as clearly evidenced in the case of iron exchanged HA [96]. Although not discussed in this study, in the absence of detectable modification of the XRD patterns, the increasing broadness of the NMR signal with increasing Co loading might be induced by long range perturbations induced by the presence of surface paramagnetic Co^{2+} ions. Using a similar preparation method starting from calcium HA, Bozon Verduraz et coll. concluded to surface cation exchange and estimated that the Co^{2+}/Ca^{2+} level of exchange was limited to 1.35 wt% Co(**Figure 8B)** [10].

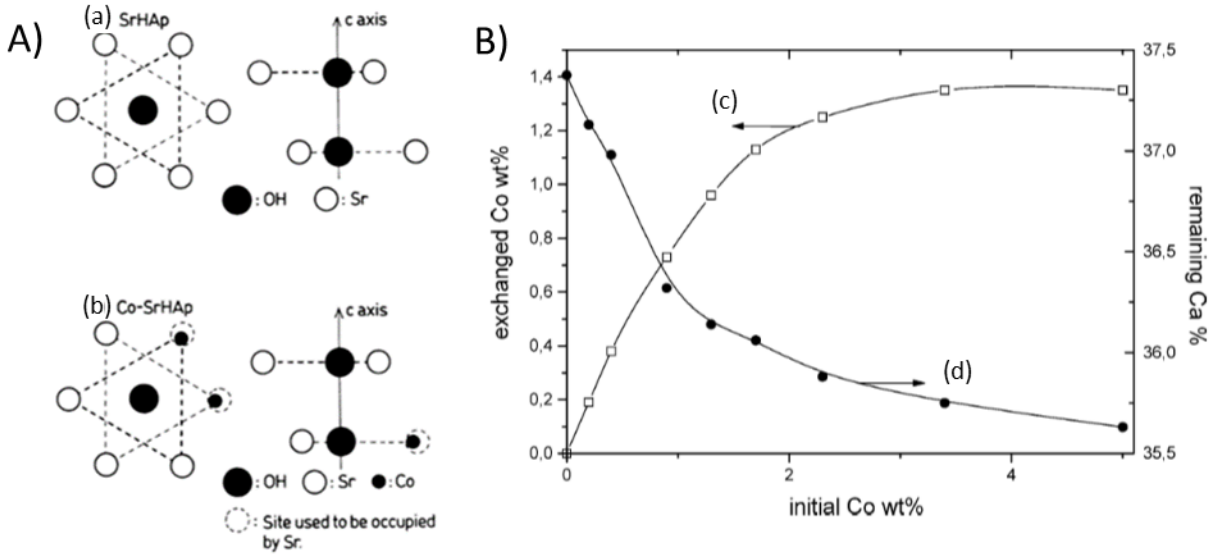

Figure 8: A) Schematic illustration of local structure of SrHA (a) and Co-SrHA (b). Source: [95]. Adapted with permission of Elsevier), B) Amounts of exchanged cobalt (c) and remaining (d) versus initial Co content in the solution. Source: [10]. Adapted with permission of Elsevier.

Given that no oxidation to Co^{3+} was observed even upon thermal treatment up to 550°C in air (the maximum reaction temperature), a marked support effect was emphasized: the apatite matrix impedes the oxidation of Co^{2+} [10]. Indeed, according to magnetic studies, the cobalt remains highly dispersed as paramagnetic isolated Co^{2+} ions. Upon impregnation method, cobalt was also found to be first exchanged with Ca^{2+} as isolated Co^{2+} for cobalt loading ≤ 0.9 wt% [97]. The additional formation of Co_xO_y clusters, then of Co_3O_4 nanocrystals was induced as cobalt loading increases as summarized in **Figure 9** [97].

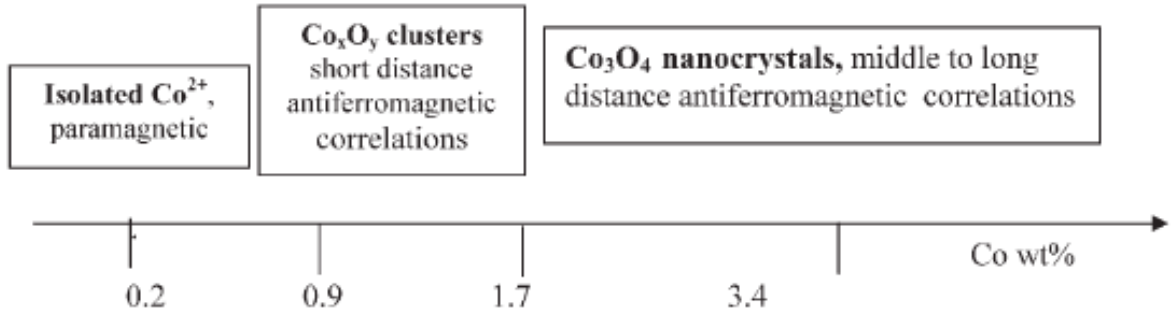

Figure 9: Co species appearing upon increasing the Co content deposited by impregnation method. Source: [97]. Adapted with permission of the Royal Society of Chemistry.

Sugiyama reported first that over Co-SrHA, the conversion of propane, the selectivity to propylene, and the reaction rate per unit of the corresponding surface area increased upon increasing incorporation of Co^{2+} as isolated exchanged ions (**Table 2,** entry 6) [95]. Such

beneficial impact of isolated Co^{2+} species was confirmed for the ODHE reaction on Co-HA [10, 97]. In the case of exchanged samples, the ethylene yield reaches a maximum (21%) for ~1 wt% Co at 550°C (**Table 2**, entry 9) [10]. Consistently, high cobalt loaded catalysts prepared by impregnation methods (involving Co_xO_y then Co_3O_4, **Figure 9**) were found much less active than those involving isolated Co^{2+} ions only prepared at lower loadings [97]. Note that the maximum yield of ethylene observed for a given reaction temperature was higher for the exchanged samples than for the impregnated ones (21.3% against 16.6% at 550°C, **Figure 10**). This was ascribed to the lower exchange capacity when depositing surface cobalt species in impregnation conditions. The maxima observed were explained by the involvement of different Co^{2+} sites depending on Co content, the isolated cobalt cations (as Co^{2+}-O-Ca^{2+}) being found more efficient than polymeric ones.

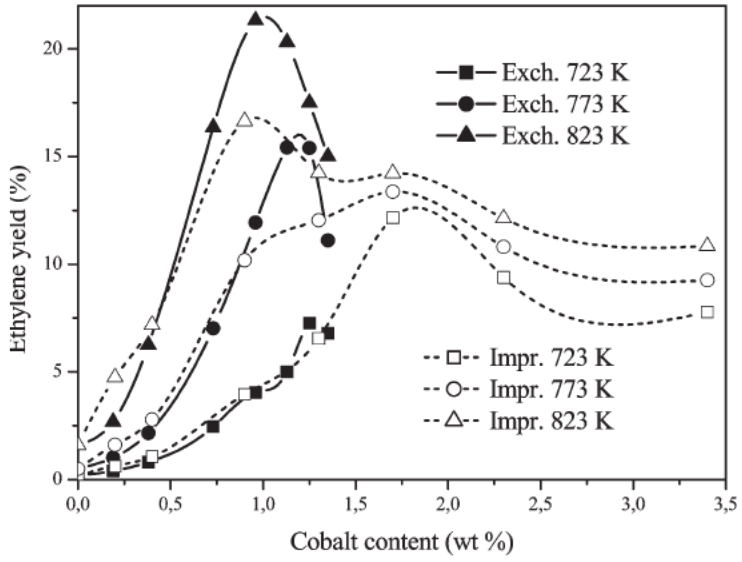

Figure 10: Comparison of ethylene yields measured at various reaction temperatures on cobalt-hydroxyapatite samples prepared by cation exchange and impregnation methods. Source: [97]. Adapted with permission of the Royal Society of Chemistry.

Interestingly, the occurrence of similar maxima was observed in the butan-2-ol model reaction that almost exclusively led to butanone upon dehydrogenation route. The involvement of active basic oxygen derived from the abstraction of hydrogen from OH groups was thus proposed (see section 3.2.3). The maximum observed was explained by a compensation of two parameters, the intrinsic dehydrogenating activity first provided by cobalt and the decrease in basicity of apatite induced by the replacement of Ca^{2+} by Co^{2+} (decrease of basicity of bridging oxygen atoms).

Trivalent iron and chromium cations

High alkene selectivities were previously reported in the presence of iron-containing phosphates for various dehydrogenation reactions [15, 105, 106]. From previous studies of chromium supported catalysts for the ODHP reaction, the 'Cr^{3+} clusters' were proposed to be involved as active centers for the ODHP reaction, although this point still remained controversial [107-110]. This question prompted Zyiad et coll. to consider chromium and iron exchanged hydroxyapatite for the ODHP reaction (**Table 2**, entries 7, 8). The impregnation method was only tested in the case of the isobutane oxidative dehydrogenation (**Table 2**, entry 11) [98]. Although not tested in comparable conditions for the ODHP reaction, the iron or chromium exchanged systems appeared less performant than the cobalt modified one (**Table 2,** entry 6). However, these studies also clearly emphasized the beneficial role of isolated metal cations [5, 96].

In line with the acidity of the metal solution, the occurrence of a dissolution precipitation process during the ion exchange procedure was clearly evidenced for iron hydroxyapatite, which explains the significant modification of the specific surface areas of the resulting materials compared to that of the support [95]. Moreover, in the context of exchange of Ca^{2+} ions by trivalent cations, the question of the charge balance is a key issue. In fact, the extent of the Ca^{2+}/M^{3+} exchange was expected to depend on the nature and charge of the metal species predominant in solution. While formally exchanged as $[Fe(H_2O)_5(OH)]^{2+}$or $[Cr(H_2O)_5(OH)]^{2+}$ complexes present in the precursor solutions at pH 2.3 and 4.8, respectively [5, 96], only isolated Fe^{3+} and Cr^{3+} cations were finally obtained upon subsequent calcination. Note that the oxidability of the exchanged Cr^{3+} ions was found to be limited to the lowest Cr content [5], and Cr^{6+} species, detected at very low metal loading, were finally found to be rapidly reduced by the reaction feed. For both metals, the charge balance associated with Ca^{2+}/M^{3+} exchange in the calcined samples was proposed to be adjusted by the removal of protons. As Fe loading increases, the increasing intensity of the visible absorption band at 850-910 nm shows there is an agglomeration of iron species, which is detrimental for propene yield (**Figure 11**). In addition, due to the correlation observed between the ODHP and the butanol conversion to butanone, the basicity was considered to be a key parameter to rationalize the performance. It was once again concluded that the M^{3+}-O-Ca^{2+} sites generated at low metal loading provide a reasonable performance in propane ODH, most likely because they maintain the needed basicity for the hydrogen abstraction from the propane. On the contrary, the limitation observed for

higher metal content was explained by the decreased basicity induced by additional fixation of M^{3+} as M^{3+}-O-M^{3+} [5, 96].

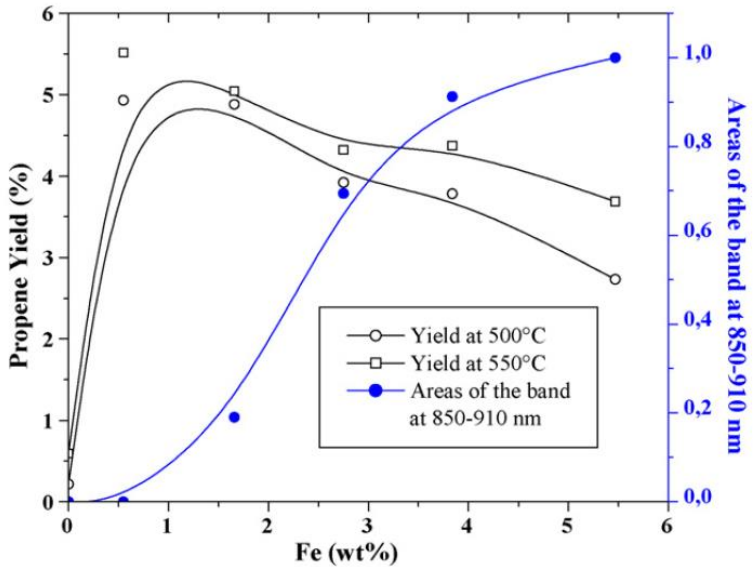

Figure 11: Comparison of yields obtained for Fe(x)/HA with the areas of the band at 850-910 nm *versus* Fe loading (blue curve). Source:[96]. Adapted with permission of Elsevier.

In the case of isobutane oxidative dehydrogenation reaction, undoped hydroxyapatites were reported to be moderately active and selective. The higher performance obtained for stoichiometric HA than for under-stoichiometric ones once more supports that basic sites are essential to catalyze the ODH reaction [98]. Upon deposition of increasing loadings of chromium by impregnation, despite improvement of isobutane conversion, the selectivity to isobutene was greatly decreased, probably due the formation of chromium oxide [98]. Such a tendency confirms that isolated cationic species are favorable to this class of reaction and that this configuration is better controlled upon cation exchange.

3.2.2.2 Modifications by vanadate anions

Vanadium based systems have been extensively studied for the oxidative dehydrogenation of propane and VMgO is a well-known reference catalyst for this reaction [8, 11, 72]. Among magnesium vanadates, $Mg_2V_2O_7$ is generally accepted as the most active phase. It was suggested that the V=O and/or V-O-V bonds participate to the activation of propane and that the activity may be related to the easy abstraction of lattice oxygen [11, 79].

Modifications of hydroxyapatites by vanadate anions have been achieved by both one-pot coprecipitation (**Table 2**, entries 1, 4, 5) and impregnation in excess of solution (**Table 2**, entry

2, 3). Sugiyama et coll. first investigated the coprecipitation synthesis, but in their operating conditions, they reported that the limit of vanadium incorporation by substitution was quite low (V/P 0 → 0.15) [86]. Promising performance, close to those reached for the $Mg_2V_2O_7$ phase under the same reaction conditions (14.0% conversion and 51% propylene selectivity), were reported for the V/P = 0.1 composition (**Table 2,** entry 1). The authors proposed that the combination of VO_4 groups and active sites of hydroxyapatite (see section 3.2.3) may be involved. They also emphasized the interesting redox properties of vanadate-substituted calcium hydroxyapatite: the reduction of V^{5+} to V^{4+} in the used catalysts was illustrated by the drastic decrease of the ^{51}V solid state NMR signal (that only probes V^{5+} species) and the initial signal could be easily regenerated in presence of oxygen at 450°C [86]. Costentin et coll. recently showed that thanks to peculiar attention devoted to the constant control of the pH during precipitation, vanadium could be successfully incorporated in the full range of the solid solution, $Ca_{10}(VO_4)_x(PO_4)_{6-x}(OH)_2$ (x 0→ 6) with Ca/P+V = 1.66 [85]. Within this series of compounds an optimal propylene yield was observed for x = 5.22 (**Table 2**, entry 4). Unfortunately, despite such high bulk vanadium loading, XPS analyses and adsorption of CO probe molecule (likely to detect surface acidic vanadium species) showed that vanadate tetrahedra are deeply relaxed inside the surface layer, which may explain that the performance obtained remained limited [87].

In contrast with the coprecipitation approach, wet impregnation over CaHA, SrHA and BaHA allowed to vary at purpose the surface vanadium content [93, 94]. Under the same reaction conditions, T_R = 450°C, $P(C_3H_8)/P(O_2)$= 3.5, W/F= 16.7 mg min^{-1} mL^{-1}, the order of both propane conversion and propene selectivity was the following VO_x /SrHA > VO_x /CaHA > VO_x /BaHA (**Table 2,** entries 2, 3) [93, 94]. The poor performance obtained for the barium system was ascribed too weak interactions of vanadate on the corresponding support whereas the peculiar redox properties of the strontium system would be responsible for its better properties [94]. From **Table 2 (**entries 2, 3), both the nature of the alkaline earth cation and the vanadium content greatly impact the specific area [93, 94]. It is found to decrease as V loadings increase. It is questionable if dissolution precipitation, likely to hinder the accessibility of vanadium on the surface might be favored as the vanadium loading increased. In addition, Friedrich *et coll.* observed similar decrease of specific surface areas on the vanadium impregnated hydroxyapatites (Ca, Sr, Mg, Ba) and they mentioned that corresponding pyrovanadate phase was formed in the as prepared samples for V_2O_5 weight loading higher than 10% (corresponding to 3 wt% V loading, **Table 2,** entries 12, 13) [89-91]. They evaluated the

performance of these catalysts for *n*-heptane or *n*-octane oxidative dehydrogenation reactions (**Table 2**, entries, 12-14) [89-92]. The vanadium pentoxide, which is the dominant dispersed phase in the lower loading (2.5 wt% in V_2O_5, corresponding to 0.7 wt% in vanadium) gave high selectivity towards octenes and low selectivity towards aromatics [90]. At higher loading, due to the presence of pyrovanadate phase, the octene selectivity was decreased at benefit of the formation of secondary mild oxidation products, C8 aromatics and oxygenates [90, 99]. The nature of the alkaline earth cation influences the products distributions, and highest selectivity to octane, aromatics or oxygenates were obtained for calcium, strontium and magnesium hydroxyapatites, respectively. A possible synergistic effect due to the co-existence between the V_2O_5 and the pyrovanadate phases was proposed [99] since the highly reactive surface oxygen species of the isolated tetrahedra of the pyrovanadate phase should promote the secondary oxidation of octenes [91, 99].

Synergistic effects between vanadium substituted hydroxyapatite and $Ca_4V_4O_{14}$ phases were also shown to be responsible for the significant enhancement of the propylene selectivity compared to that obtained with pure vanadium substituted hydroxyapatite (**Table 2,** entry 5) [87, 88]. The $Ca_4V_4O_{14}$ phase alone led to very poor propane conversion. While continuous adjustment of the pH of the coprecipitation medium to 9 during the preparation led to the formation of the pure substituted hydroxyapatite, periodic base addition [85] led to the epitaxial growth of the $Ca_4V_4O_{14}$ phase onto the vanadium substituted phase [88]. Combination of HRTEM, solid state NMR and EPR studies allowed to precise the structure of the interface. The best phase cooperation obtained for the phase composition VHA : $Ca_4V_4O_{14}$: = 95 / 5 wt% corresponds to a complementary properties between the catalytic functions provided by each phase: the intrinsic ability of vanadium substituted hydroxyapatite to activate propane (see section 3.2.3) and the easier electron delocalization on the vanadium tetramers located at the phase's boundaries compared to monomeric vanadate present in V-HA that is beneficial to propene selectivity [88].

3.2.3 Activation site and mechanism

From the former section, the modification of hydroxyapatite by exchanged Co, Cr or Fe cations concluded that isolated cations should be favored to achieve selective activation of alkanes. On the other hand, except for vanadium impregnated samples where oxygen of the VO_x formed at the surface are able to activate the propane, isolated VO_4 tetrahedra in $Ca_{10}(VO_4)_x(PO_4)_{6-x}(OH)_2$ solid solutions incorporated by coprecipitation were found to be too poorly accessible for efficient activation of propane. This raises the question of the nature of

the active site able to activate light alkane over metal modified hydroxyapatite. Given that the limiting step is H abstraction, a beneficial influence of basicity on the activation process was proposed [84, 87, 96, 111, 112]. It is well supported by the established relationships between the alkane conversion and basic reactivity probed by model reactions [10]. The nature of basic entities able to activate alkane deserves discussion.

Due to their electrophilic properties, adsorbed active O^- and O_2^- oxygen possibly present on HA surface are expected to be associated with non-selective oxidation [70, 78]. At reverse, nucleophilic lattice O^{2-} oxide ions should be preferentially involved in the selective process. In the HA structure, among the two types of lattice oxygen species present in phosphate and hydroxyl groups, the involvement of O^{2-} from PO_4^{3-} was discarded on the basis on the much lower activity of $Ca_3(PO_4)_2$ compound compared to that of hydroxyapatite [113]. On the contrary, based on the progressive deactivation associated with the conversion of hydroxyapatite into corresponding chloroapatites in the presence of tetrachloromethane in the feed stream and to the rather low activities observed on chloroapatite [113, 114], it was inferred that hydroxyl groups must somehow participate to the activation process of light alkanes [58, 89, 95, 104]. However, hydroxyl groups being weak bases [115, 116], it was also underlined that it would be surprising that OH^- groups of HA directly contribute to hydrogen abstraction of alkanes [95, 104]. However, Sugiyama *et al.* rather assumed that OH^- of HA may be a source of active oxygen species [104]. Described as similar to lattice oxygen in oxide catalysts, based on results obtained for SrHA with and without Co^{2+} doping, they proposed that this active oxygen species would derive from OH^- by hydrogen desorption [86, 95, 104]. They studied the gas phase H-D exchangeability of hydroxyl groups of calcined hydroxyapatite by D_2O at 450°C. Solid state ^1H MAS NMR characterizations of SrHA and Co-SrHA allowed to evaluate the H-D exchangeability of OH groups following the signal at ~ 0 ppm [95, 104]. Apart a progressive decrease of the chemical shift of this peak, its intensity decreased with increasing Co^{2+} content. Although not considering some misleading effect due to the paramagnetism induced by Co^{2+}, the authors concluded to the enhancement of H-D exchangeability [95, 104]. Hydrogen abstraction ability could also be achieved with CH_3OD [117]. Although these H-D exchange experiments could not provide direct evidence for the stable presence of oxygen species that would be involved in the activation of propane, the authors underlined that the tendencies observed strongly support that active oxygen species should be formed during the catalytic reaction and that that modification of hydroxyapatite by cobalt would favor this process [95].

The generation of active O^{2-} from OH^- was later discussed in relation with intrinsic ionic conduction properties of HA [10, 87, 118, 119]. In the case of cation exchange of Ca^{2+} by trivalent cations, the OH deprotonation required to ensure the charge balance was proposed to generate Ca^{2+}-O-M^{3+}, which is able to activate propane [5, 96]. In the case of divalent Co^{2+} ions modification (introduced by cation exchange), it was hypothesized that the formation of active O^{2-} may be favored by the mobility of neighboring lattice oxygen or OH^- groups and may thus influence the activation process [10]. The authors proposed a mechanism described by Equations (1-2), where O_o is a lattice oxygen and V_o a neutral oxygen vacancy. This oxygen present in Co^{2+}-O-Ca^{2+} entities would both activate ethane and act as labile oxygen. The neutral oxygen vacancy formed upon its departure would be further replenished by gaseous oxygen [10].

$C_2H_6 + O_o \rightarrow C_2H_4 + H_2O + V_o$ (Eq. 1)

$½\ O_2 + V_o \rightarrow O_o$ (Eq. 2)

Such key role played by the bulk anisotropic conduction onto the surface reactivity was later unambiguously demonstrated by Costentin et coll. et al. to rationalize the behavior of solid solution of vanadium substituted apatite for oxidative dehydrogenation of propane thanks to combination of advanced *in situ* and *operando* characterization techniques [87]. Firstly, ^1H NMR evidenced that there was a lack of protons inside the OH columns while the vanadium was increasingly incorporated in the bulk lattice by coprecipitation achieved maintaining the pH constant to 9 value. In addition, the formation of the vanadium oxy-hydroxy-apatite $Ca_{10}(PO_4)_{6-x}(VO_4)_x(OH)_{2-2y}O_y$ solid solution was favored upon thermal treatment thanks to partial dehydration along the OH columns generating additional O^{2-} oxide ions. Their formation was also supported by *in situ* DRIFT with the appearance of a characteristic shoulder at ~3530 cm^{-1} that was ascribed to H-bonding interaction between the generated O^{2-} oxide ions and the remaining adjacent O-H groups inside the channels. These bulk O^{2-} species were found to be stable at high temperature. According to impedance spectroscopy, they initiate the activation of proton anisotropic ionic conductivity along the columns running along the *c* axis. This proton migration process eventually resulted in the exposure of surface O^{2-} species (**Figure 12)** that could act as strong basic sites. This is supported by the ability of surface Ca^{2+}-O^{2-} pairs to dissociate H_2 [87]. The key role played in the activation of propane by these strong basic O^{2-} ions was supported by the unique synergistic effect between the propane to propene catalytic reaction and the proton mobility process evidenced by *operando* impedance spectroscopy. It is shown that the transformation of propane to propene proceeds both upon oxidative dehydrogenation reaction (O_2 is required for propene formation), and dehydrogenation reaction

(minor route). Finally, based on all the collected data, a catalytic cycle for the ODHP reaction was proposed (**Figure 13**). It requires two types of surface oxygen ions: - a basic O^{2-} species emerging from the OH channels of the apatite framework and -a labile oxygen from the VO_4 tetrahedra. The former species is formed and regenerated upon the assistance of the peculiar proton conduction ability of the apatite material. The latter species can be protonated by proton diffusion and can contribute to the formation/desorption of a water molecule. This oxygen species is eventually regenerated by oxidation with gaseous oxygen.

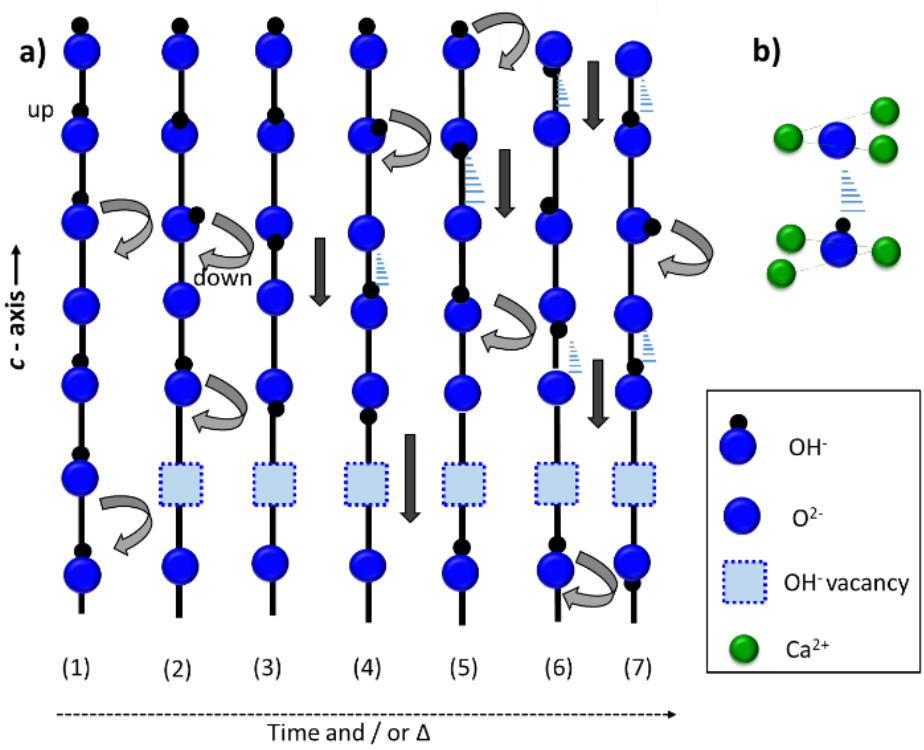

Figure 12: a) Schematic representation of the thermally-activated proton migration mechanism in the oxy-hydroxy-apatite system. This schematic representation shows (1) the stacking of OH^- along the c axis including O^{2-} native defects present in vanadium-modified apatites, and the proton rotation activated at low temperature that are favored by the polarization induced by the defective stacking, (2) O^{2-} species generated upon thermal dehydration together with a OH vacancy site, (3-7) and the proton transportation along the *c*-axis activated in the medium range temperature. The proton migration occurs from the upper layers to the lower ones with time, resulting in O^{2-}climbing up from the bulk to the surface. Slight displacement of the O^{2-} ion from the initial position of the OH^- group allows the formation of O^{2-}…HO^- H-bonding interaction. **b)** Ca^{2+} triangles coordination sphere of the OH^- and O^{2-} anions present in the channels. Source: [87]. Adapted with permission of Wiley-VCH.

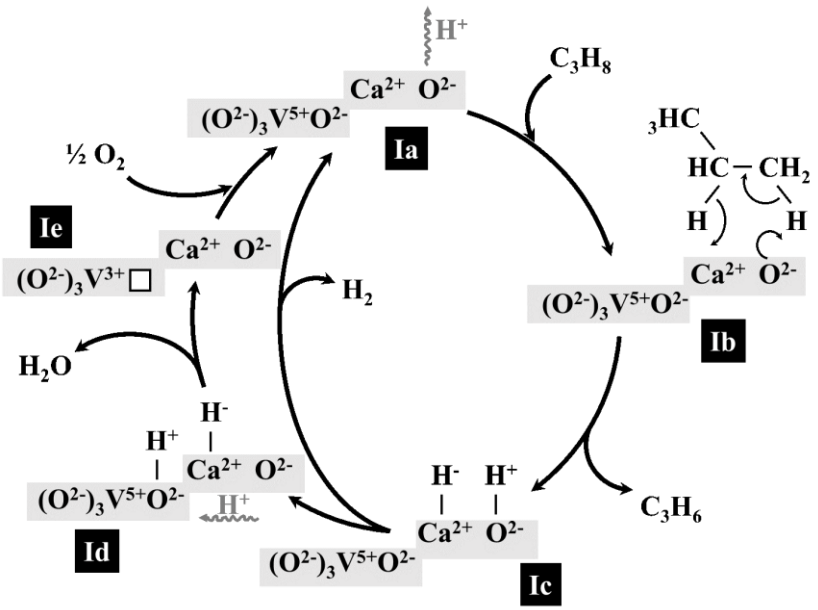

Figure 13: Schematized representation of the catalytic transformation of propane to propene involving dehydrogenation and oxidative dehydrogenation routes on V-HA samples exhibiting Ca^{2+}-O^{2-} surface acid-base pairs generated thanks to proton migration process that are close to VO_4 tetrahedra. The square box represents an oxygen vacancy and ~~~~> refers to the proton migration process. Source: [87]. Adapted with permission of Wiley-VCH.

4. Conclusions and perspectives

Metal modified hydroxyapatites have been studied since the 90's as heterogeneous catalysts for selective oxidation reactions. Very interesting results have already been reported for the oxidation of primary alcohols in the liquid phase under aerobic conditions and the partial methane oxidation operating in gas phase at very high temperature (up to 800°C). This illustrates the large application scope of the hydroxyapatite system due to its stability in a very large range of conditions.

From the analysis of the literature dealing with the selective oxidation of primary alcohols in the liquid phase under aerobic conditions over metal modified hydroxyapatite, Pd-based systems are quite interesting. Despite the higher price of Pd compared to Ru, the latter has to be used at a higher loading. Significant improvements have however been achieved in reducing the amount of Ru while maintaining good catalytic performance but complicating the catalyst synthesis procedure (addition of another metal or of organic additives). The reference substrate for aerobic oxidations of primary alcohol is clearly benzyl alcohol. It should be noted that its conversion into benzaldehyde by aerobic and heterogeneous catalysis in liquid phase is of interest because of the use of this compound as a flavoring agent, *etc.* (7000 t produced per

year in 1999 [118]. Other aldehydes of industrial importance are cinnamaldehyde, vanillin but the one that is the most industrially produced is formaldehyde because of its involvement in the synthesis of polymeric materials. Gas phase aerobic oxidation of methanol was not examined in this chapter but it can be noted that there are some reports dealing with the use of hydroxyapatite supported molybdenum oxide catalysts for this reaction [119].

Rhodium supported hydroxyapatite shows the best performance for the partial oxidation of methane. Although also very promising, the nickel catalyst obtained from coprecipitation synthesis is a complex multiphasic sample. It is thus unclear if the highly dispersed active Ni species that were extracted from the bulk to the surface during the POM reaction comes from the Ni-substituted hydroxyapatite and / or from the other Ni phosphate phase. Optimization of the precipitation conditions to get single phase Ni-hydroxyapatite would be useful to investigate this point. In addition, comparisons with the highly dispersed nickel or even isolated single Ni atoms obtained upon ion exchange and reported to be very efficient for the dry reforming of methane [64] would also be of interest.

The oxidative dehydrogenation of light alkanes into alkenes remains more challenging since the lower stability of alkenes compared to alkanes and CO_2 makes the control of alkene selectivity difficult in the presence of oxygen. Nevertheless, quite promising results have been reported with the vanadium system for propane conversion to propene, with performances very comparable to those of a well-known reference catalyst. Cobalt exchanged hydroxyapatite also shows good selectivity for the oxidative dehydrogenation of ethane.

For all the investigated systems, further optimization requires better control of the synthesis and advanced characterizations allowing to establish fine structure-reactivity relationships. In particular, better description of the role played by the hydroxyapatite itself in the selective oxidation reactions is of peculiar interest.

In most studies, hydroxyapatite was mainly envisaged as a support for the dispersion of the active phase. The formation of highly dispersed metal sites is favoured due to the peculiar ability of the hydroxyapatite structure for substitution and it can be achieved either by one step coprecipitation procedure, or by post synthesis cation exchange in the excess of solution. Wet impregnation approach may also lead to highly dispersed species, but non-selective oxide like active phase could be preferentially obtained for high metal loadings. This may explain that an optimum metal loading was often identified, namely for Co impregnated system for the ODHE reaction. Better attention should also be devoted to the control of dissolution precipitation of the support possibly occurring in acid conditions imposed by the metal salt containing solution

since such process may be detrimental to the specific surface area and to the metal accessibility onto the surface. Although reported efficient for vanadium-substituted hydroxyapatite, coprecipitation is a priori less favourable in terms of economy of metal atoms. Moreover, as mentioned above, depending on the metal, the formation of single phased metal-hydroxyapatite is not easy to monitor. Note however, that, as sometimes described for other systems also governed by the Mars and Van Krevelen mechanism, beneficial synergistic effects resulting from the complementary functions provided by each phase were finally observed for a vanadate tetrameric phase grown onto a vanadium substituted hydroxyapatite.

Beside the control of the metal dispersion, hydroxyapatite is an original support with modulating acid-base properties that can be monitored by varying its stoichiometry and/ or by substituting calcium by other alkaline earth cations. As far as aerobic oxidation of alcohol reaction is concerned, although the authors preferentially used stoichiometric hydroxyapatite, known to exhibit basic properties, there is no mention of the possible involvement of the basic sites of apatite itself. Note however that the authors point out that the Ru or Pd/apatite catalytic systems avoid the use of any additional base. It could be interesting to investigate if the basic properties of the hydroxyapatite itself take part in the liquid phase oxidation reactions. The direct involvement of the hydroxyapatite as part of the active phase was more directly discussed in the case of alkane oxidative dehydrogenation reactions. Similar tendencies were reported between the basic reactivity evaluated by a model reaction and the ODH activity. Rather than OH groups that are too weak bases, their derived O^{2-} form, that are *in situ* generated *via* the thermally activated proton ionic conduction process, have been shown to be much stronger basic sites and to be involved in the activation of the C-H bond of propane. Such role played by basic sites of hydroxyapatite in the ODH mechanism illustrates that metal modified hydroxyapatite system are original and can be very efficient bifunctional redox and acid-base catalysts.

REFERENCES

1. Parmeggiani C, Cardona F. (2012). Transition metal based catalysts in the aerobic oxidation of alcohols. *Green Chem*. 14:547-64.
2. Boukha Z, Gil-Calvo M, de Rivas B, González-Velasco JR, Gutiérrez-Ortiz JI, López-Fonseca R. (2018). Behaviour of Rh supported on hydroxyapatite catalysts in partial oxidation and steam reforming of methane: On the role of the speciation of the Rh particles. *Appl Catal A*. 556:191-203.
3. Jiménez-González C, Boukha Z, de Rivas B, Delgado JJ, Cauqui MA, González-Velasco JR, et al. (2013). Catalytic Performance of $Ni/CeO_2/X\text{-}ZrO_2$ (X = Ca, Y) Catalysts in the Aqueous-Phase Reforming of Methanol. *Appl Catal A.* 466:9-20.
4. Dong S, Altvater NR, Mark LO, Hermans I. (2021). Assessment and comparison of ordered & non-ordered supported metal oxide catalysts for upgrading propane to propylene. *Appl Catal A*. 617:118121.
5. Boucette C, Kacimi M, Ensuqye A, Piquemal JY, Bozon-Verduraz F, Ziyad M. (2009). Oxidative dehydrogenation of propane over chromium-loaded calcium-hydroxyapatite. *Appl Catal A.* 256:201-10.
6. Cavani F, Trifiro F. (1999). Selective oxidation of light alkanes: interaction between the catalyst and the gas phase on different classes of catalytic materials. *Catal Today.* 51:561-80.
7. Centi G, Cavani F, Trifiro F. (2001). Selective Oxidation by Heterogeneous Catalysis. Publishers KAP, editor.
8. Cavani F. (2010). Catalytic selective oxidation: The forefront in the challenge for a more sustainable chemical industry. *Catal Today*. 157(1):8-15.
9. Cortez Corberan V. (2009). Nanostructured Oxide Catalysts for Oxidative Activation of Alkanes. *Top Catal.* 52:962–9.
10. Elkabouss K, Kacimi M, Ziyad M, Ammar S, Bozon-Verduraz F. (2004). Cobalt-exchanged hydroxyapatite catalysts: magnetic studied, spectroscopic investigations, performance in 2-butanol and ethane oxidative dehydrogenations. *J Catal.* 226:16-24.
11. Carrero CA, Schloegl R, Wachs IE, Schomaecker R. (2014). Critical Literature Review of the Kinetics for the Oxidative Dehydrogenation of Propane over Well-Defined Supported Vanadium Oxide Catalysts. *ACS Catal*. 4:3357-80.
12. Concepción P, Blasco T, López Nieto JM, Vidal-Moya A, Martínez-Arias A. (2004). Preparation, characterization and reactivity of V- and/or Co-containing AlPO-18 materials (VCoAPO-18) in the oxidative dehydrogenation of ethane. *Microporous and Mesoporous Mater.* 67(2):215-27.

13. Savary L, Saussey J, Costentin G, Bettahar MM, Gubelmann-Bonneau M, Lavalley JC. (1996). Propane oxydehydrogenation reaction on a VPO/TiO_2 catalyst. Role of the nature of acid sites determined by dynamic in situ IR studies. *Catal Today.* 32:57-61.
14. Savary L, Saussey J, Costentin G, Bettahar MM, Lavalley JC, Gubelmann-Bonneau M. (1996). Role of the nature of the acid sites in the oxydehydrogenation of propane on a VPO/TiO_2 catalyst. An *in situ* FT-IR spectroscopy investigation. *Catal Lett.* 38:197-201.
15. Millet JMM, Védrine JC. (2001). Importance of site isolation in the oxidation of isobutyric acid to methacrylic acid on iron phosphate catalysts. *Top Catal.* 15(2-4):139-44.
16. Grasselli RK. (2014). Site isolation and phase cooperation: Two important concepts in selective oxidation catalysis: A retrospective. *Catal Today.* 238:10-27.
17. Callahan JL, Grasselli RK. (1963). A selectivity factor in vapor-phase hydrocarbon oxidation catalysis. *AIChE J*. 9(6):755-60.
18. Singh RP, Bañares MA, Deo G. (2005). Effect of phosphorous modifier on V_2O_5/TiO_2 catalyst: ODH of propane. *J Catal.* 233(2):388-98.
19. Centi G, Trifirò F, Busca G, Ebner J, Gleaves J. (1989). Nature of active species of $(VO)_2P_2O_7$ for selective oxidation of *n*-butane to maleic anhydride. *Faraday Disc Chem Soc.* 87(0):215-25.
20. Wang Y, Otsuka K. (1997). Partial Oxidation of Ethane by Reductively Activated Oxygen over Iron Phosphate Catalyst. *J Catal.* 171:106-14.
21. Savary L, Costentin G, Maugé F, Lavalley JC, El Fallah J, Studer F, et al. (1997). Characterization of $AgMo_3P_2O_{14}$ Catalyst Active in Propane Mild Oxidation. *J Catal.* 169(1):287-300.
22. Savary L, Costentin G, Bettahar MM, Lavalley JC, Boudin S, Grandin A, et al. (1996). Structure-sensitivity study of partial propene oxidation over $AV_2P_2O_{10}$ vanadium phosphate compounds. *J Chem Soc, Faraday Trans.* 92(8):1423-8.
23. Costentin G, Savary L, Lavalley JC, Borel MM, Grandin A. (1998). Structural Effects on Propane Mild Oxidation from Comparative Performances of Molybdenum and Vanadium Phosphate Model Catalysts. *Chem Mater.* 10(1):59-64.
24. Savary L, Costentin G, Bettahar MM, Grandin A, Gubelmann-Bonneau M, Lavalley JC. (1996). Effects of the structural and cationic properties of $AV_2P_2O_{10}$ solids on propane selective oxidation. *Catal Today.* 32:305-9.
25. Sheldon RA. (2017). The E factor 25 years on: the rise of green chemistry and sustainability. *Green Chem.* 19:18-43.
26. Alfonsi K, Colberg J, Dunn PJ, Fevig T, Jennings S, Johnson TA, et al. (2008). Green chemistry tools to influence a medicinal chemistry and research chemistry based organization. *Green Chem.* 10:31-6.
27. Gunasekaran N. (2015). Aerobic Oxidation Catalysis with Air or Molecular Oxygen and Ionic Liquids. *Adv Synth Catal.* 357:1990-2010.

28. Cornell CN, Sigman MS. (2007). Recent Progress in Wacker Oxidations: Moving toward Molecular Oxygen as the Sole Oxidant. *Inorg Chem.* 46:1903-9.
29. Centi G, Cavani F, Trifirò F. (2012). Selective Oxidation by Heterogeneous Catalysis. Media SSB, editor.
30. Woo Lee H, Nam H, Han GH, Cho YH, Yeo BC, Kim MC, et al. (2021). Solid-solution alloying of immiscible Pt and Au boosts catalytic performance for H_2O_2 direct synthesis. *Acta Materialia*. 205:116563.
31. Yamaguchi K, Mori K, Mizugaki T, Ebitani K, Kaneda K. (2000). Creation of a Monomeric Ru Species on the Surface of Hydroxyapatite as an Efficient Heterogeneous Catalyst for Aerobic Alcohol Oxidation. *J Am Chem Soc.* 122:7144-5.
32. Shaabani A, Afaridoun H, Shaabani S. (2016). Natural hydroxyapatite-supported MnO_2: a green heterogeneous catalyst for selective aerobic oxidation of alkylarenes and alcohols. *Appl Organomet Chem.* 30:772-6.
33. Shaabani A, Shaabani S, Afaridoun H. (2016). Highly selective aerobic oxidation of alkyl arenes and alcohols: cobalt supported on natural hydroxyapatite nanocrystals. *RSC Adv.* 6(54):48396-404.
34. Opre Z, Grunwaldt JD, Mallat T, Baiker A. (2005). Selective oxidation of alcohols with oxygen on Ru-Co-hydroxyapatite: A mechanistic study. *J Mol Catal* 242(1-2):224-32.
35. Opre Z, Grunwaldt JD, Maciejewski M, Ferri D, Mallat T, Baiker A. (2005). Promoted Ru–hydroxyapatite: designed structure for the fast and highly selective oxidation of alcohols with oxygen. *J Catal*. 230:406-19.
36. Opre Z, Ferri D, Krumeich F, Mallat T, Baiker A. (2006). Aerobic oxidation of alcohols by organically modified ruthenium hydroxyapatite. *J Catal.* 241(2):287-95.
37. Mori K, Kanai S, Hara T, Mizugaki T, Ebitani K, Jitsukawa K, et al. (2007). Development of Ruthenium-hydroxyapatite-encapsulated superparamagnetic γ-Fe_2O_3 nanocrystallites as an efficient oxidation catalyst by molecular oxygen. *Chem Mater.* 19:1249-56.
38. Mori K, Yamaguchi K, Hara T, Mizugaki T, Ebitani K, Kaneda K. (2002). Controlled Synthesis of Hydroxyapatite-Supported Palladium Complexes as Highly Efficient Heterogeneous Catalysts. *J Am Chem Soc.* 124(39):11572-3.
39. Mori K, Hara T, Mizugaki T, Ebitani K, Kaneda K. (2004). Hydroxyapatite-Supported Palladium Nanoclusters: A Highly Active Heterogeneous Catalyst for Selective Oxidation of Alcohols by Use of Molecular Oxygen. *J Am Chem Soc.* 126(34):10657-66.
40. Jamwal N, Gupta M, Paul S. (2008). Hydroxyapatite-supported palladium (0) as a highly efficient catalyst for the Suzuki coupling and aerobic oxidation of benzyl alcohols in water. *Green Chem.* 10(9):999-1003.
41. Sugiyama S, Minami T, Hayashi H, Tanaka M, Shigemoto N, Moffat JB. (1996). Enhancement of the selectivity to carbon monoxide with feedstream doping by tetrachloromethane in the

oxidation of methane on stoichiometric calcium hydroxyapatite. *J Chem Soc Faraday Trans.* 92(2):293-9.

42. Kaneda K, Mizugaki T. (2009). Development of concerto metal catalysts using apatite compounds for green organic syntheses. *Energy Environ Sci.* 2:655-73.
43. Abad A, Almela C, Corma A, García H. (2006). Efficient chemoselective alcohol oxidation using oxygen as oxidant. Superior performance of gold over palladium catalysts. *Tetrahedron Lett.* 62:6666-72.
44. Kaneda K, Mori K, Hara T, Mizugaki T, Ebitani K. (2004). Design of hydroxyapatite-bound transition metal catalysts for environmentally-benign organic syntheses. *Catal Surveys from Asia.* 8:231-9.
45. Matsumoto M, Watanabe N. (1984). Oxidation of allylic alcohols to unsaturated carbonyl compounds by ruthenium dioxide and dioxygen/ruthenium dioxide. *J Org Chem.* 49:3435-6.
46. Kaneda K, Mizugaki T. (2017). Design of High-Performance Heterogeneous Catalysts using Apatite Compounds for Liquid-Phase Organic Syntheses. *ACS Catal.* 7:920-35.
47. Lempers HEB, Sheldon RA. (1998). The Stability of Chromium in CrAPO-5, CrAPO-11, and CrS-1 during Liquid Phase Oxidations. *J Catal.* 175:62-9.
48. Mars P, van Krevelen DW. (1954). Oxidations Carried out by means of Vanadium Oxide Catalysts. *Chem Eng Sci.* 3:41.
49. El Shafei GMS, Moussa NA. (2021). Adsorption of Some Essential Amino Acids on Hydroxyapatite. *J Colloid Interface Sci.* 238:160-6.
50. Moody CJ, Palmer FN. (2002). Dirhodium(II) carboxylate-catalysed oxidation of allylic and benzylic alcohols. *Tetrahedron Lett.* 43:139-41.
51. Muldoon J, Brown SN. (2002). Practical Os/Cu-cocatalyzed air oxidation of allyl and benzyl alcohols at room temperature and atmospheric pressure. *Org Lett.* 4:1043-5.
52. Martín SE, Suárez DF. (2002). Catalytic aerobic oxidation of alcohols by $Fe(NO_3)_3$-$FeBr_3$. *Tetrahedron Lett.* 43:4475-9.
53. Vinod CP, Wilson K, Lee AF. (2011). Recent advances in the heterogeneously catalysed aerobic selective oxidation of alcohols. *J Chem Technol Biotechnol.* 86:161-71.
54. Kaneda K, Ebitani K, Mizugaki T, Mori K. (2006). Design of high-performance heterogeneous metal catalysts for green and sustainable chemistry. *Bull Chem Soc Jpn.* 79:981-1016.
55. Davis SE, Ide MS, Davis RJ. (2013). Selective oxidation of alcohols and aldehydes over supported metal nanoparticles. *Green Chem.* 15:17-45.
56. Chen J, Zhang Q, Wang Y, Wan H. (2008). Size-dependent catalytic activity of supported palladium nanoparticles for aerobic oxidation of alcohols. *Adv Synth Catal.* 350:453-64.
57. Matsumura Y, Sugiyama S, Hayashi H, Moffat JB. (1995). An Apparent Ensemble Effect in the Oxidative Coupling of Methane on Hydroxyapatites with Incorporated Lead. *Catal Lett.* 30(1-4):235-40.

58. Sugiyama S, Iguchi Y, Minami T, Hayashi H, Moffat JB. (1997). Partial oxidation of methane to methyl chloride with tetrachloromethane on strontium hydroxyapatites ion-exchanged with lead. *Catal Lett.* 46(3-4):279-85.
59. Sugiyama S, Minami T, Moriga T, Hayashi H, Koto K, Tanaka M, et al. (1996). Surface and bulk properties, catalytic activities and selectivities in methane oxidation on near-stoichiometric calcium hydroxyapatites. *J Mater Chem.* 6(3):459-64.
60. Oh SC, Xu J, Tran DT, Liu B, Liu D. (2018). Effects of Controlled Crystalline Surface of Hydroxyapatite on Methane Oxidation Reactions. *ACS Catal.* 8(5):4493-507.
61. Boukha Z, Kacimi M, Ziyad M, Ensuque A, Bozon-Verduraz F. (2007). Comparative study of catalytic activity of Pd loaded hydroxyapatite and fluoroapatite in butan-2-ol conversion and methane oxidation. *J Mol Catal A.* 270(1):205-13.
62. Zhang Y, Zhu J, Li S, Xiao Y, Zhan Y, Wang X, et al. (2020). Rational design of highly H_2O- and CO_2-tolerant hydroxyapatite-supported Pd catalyst for low-temperature methane combustion. *ChemEng J.* 396:125225.
63. Boukha Z, Kacimi M, Pereira MFR, Faria JL, Figueiredo JL, Ziyad M. (2007). Methane dry reforming on Ni loaded hydroxyapatite and fluoroapatite. *Appl Catal A.* 317(2):299-309.
64. Akri M, Shu Zhao S, Li X, Zang K, Lee AF, Isaacs MA, et al. (2019). Atomically dispersed nickel as coke-resistant active sites for methane dry reforming. Nat Commun. 10(1):1-10.
65. Jun JH, Lee T-J, Lim TH, Nam S-W, Hong S-A, Yoon KJ. (2004). Nickel–calcium phosphate/hydroxyapatite catalysts for partial oxidation of methane to syngas: characterization and activation. *J Catal.* 221(1):178-90.
66. Choudhary VR, Uphade BS, Mamman AS. (1997). Oxidative Conversion of Methane to Syngas over Nickel Supported on Commercial Low Surface Area Porous Catalyst Carriers Precoated with Alkaline and Rare Earth Oxides. *J Catal.* 172:281-93.
67. Liu ZW, Jun KW, Roh HS, Park SE, Oh YS. (2002). Partial Oxidation of Methane over Nickel Catalysts Supported on Various Aluminas. *Korean J Chem Eng.* 19(5):735-41.
68. Lee SJ, Jun JH, Lee S-H, Yoon KJ, Lim TH, Nam S-W, et al. (2002). Partial oxidation of methane over nickel-added strontium phosphate. *Appl Catal A.* 230(1):61-71.
69. Jun JH, Lim TH, Nam SW, Hong SA, Yoon KJ. (2006). Mechanism of partial oxidation of methane over a nickel-calcium hydroxyapatite catalyst. *Appl Catal A.* 312:27-34.
70. Blasco T, Lopez Nieto JM. (1997). Oxidative dehydrogenation of short chain alkanes on supported vanadium oxide catalysts. *Appl Catal A.* 157:117-42.
71. Grabowski R. (2006). Kinetics of Oxidative Dehydrogenation of C2-C3 Alkanes on Oxide Catalysts. *Catal Rev.* 48(2):199-268.
72. Cavani F, Ballarini N, Cericola A. (2007). Oxidative dehydrogenation of ethane and propane: How far from commercial implementation? *Catal Today.* 127:113-31.

73. Kube P, Frank B, Wrabetz S, Krohnert J, Havecker M, Velasco-Velez J, et al. (2017). Functional Analysis of Catalysts for Lower Alkane Oxidation. *ChemCatChem.* 9:573–85.
74. Airaksinen SMK, Bañares MA, Krause AOI. (2005). *In situ* characterisation of carbon-containing species formed on chromia/alumina during propane dehydrogenation. *J Catal.* 230(2):507-13.
75. Fuchs S, Leveles L, Seshan K, Lefferts L, Lemonidou A, Lercher JA. (2001). Oxidative dehydrogenation and cracking of ethane and propane over LiDyMg mixed oxides. *Top Catal.* 15(2-4):169-74.
76. Kung HH. (1994). Oxidative Dehydrogenation of Light (C2 to C4) Alkanes. Eley DD, Pines H, Haag WO, editors: Academic Press. 1994/01/01/. 1-38 p.
77. Klisinska A, Samson K, Gressel I, Grzybowska GB. (2006). Effect of additives on properties of V_2O_5/SiO_2 and V_2O_5/MgO catalysts I. Oxidative dehydrogenation of propane and ethane. *Appl Catal A.* 309:10-6.
78. Banares MA. (1999). Supported metal oxide and other catalysts for ethane conversion: a review. *Catal Today.* 51:319-48.
79. Barman S, Maity N, Bhatte K, Ould-Chikh S, Dachwald O, Haeßner C, et al. (2016). Single-Site VOx Moieties Generated on Silica by Surface Organometallic Chemistry: A Way To Enhance the Catalytic Activity in the Oxidative Dehydrogenation of Propane. *ACS Catal.* 6:5908-21.
80. Chalupka K, Thomas C, Millot Y, Averseng F, Dzwigaj S. (2013). Mononuclear pseudo-tetrahedral V species of VSiBEA zeolite as the active sites of the selective oxidative dehydrogenation of propane. *J Catal.* 305:46-55.
81. Cheng MJ, Chenoweth K, Oxgaard J, van Duin A, Goddard A. (2007). Single-Site Vanadyl Activation, Functionalization, and Reoxidation Reaction Mechanism for Propane Oxidative Dehydrogenation on the Cubic V_4O_{10} Cluster. *J Phys Chem C.* 111:5115-27.
82. Corma A, Lopez-Nieto JM, Paredes N. (1993). Influence of the preparation methods of V-Mg-O catalysts on their catalytic properties for the oxidative dehydrogenation of propane. *J Catal.* 144:425-3.
83. Védrine JC. (2002). The role of redox, acid–base and collective properties and of cristalline state of heterogeneous catalysts in the selective oxidation of hydrocarbons. *Top Catal.* 21(1-3):97-106.
84. Klisinska A, Loridant S, Grzybowska B, Stocha J, Gressel I. (2006). Effect of additives on properties of V_2O_5/SiO_2 and V_2O_5/MgO catalysts II. Structure and physicochemical properties of the catalysts and their correlations with oxidative dehydrogenation of propane and ethane. *Appl Catal A.* 309:17-26.
85. Petit S, Gode T, Thomas C, Dzwigaj S, Millot Y, Brouri D, et al. (2017). Incorporation of Vanadium in the Framework of Hydroxyapatites: Importance of the Vanadium Content and pH Conditions during the Precipitation Step. *Phys Chem Chem Phys.* 19:9630 – 40.

86. Sugiyama S, Osaka T, Hirata Y, Sotowa KI. (2006). Enhancement of the activity for oxidative dehydrogenation of propane on calcium hydroxyapatite substituted with vanadate. *Appl Catal A.* 312:52-8.
87. Petit S, Thomas C, Millot Y, Krafft JM, Laberty-Robert C, Costentin G. (2020). Activation of C-H Bond of Propane by Strong Basic Sites Generated by Bulk Proton Conduction on V-Modified Hydroxyapatites for the Formation of Propene. *ChemCatChem.* 12 2506–21.
88. Petit S, Thomas C, Millot Y, Averseng F, Brouri D, Kraftt JM, et al. (2021). Synergistic Effect Between $Ca_4V_4O_{14}$ and Vanadium-Substituted Hydroxyapatite in the Oxidative Dehydrogenation of Propane. *ChemCatChem.* in press http://dx.doi.org/10.1002/cctc.202100807
89. Dasireddy VDBC, Singh S, Friedrich HB. (2015). Effect of the Support on the Oxidation of Heptane Using Vanadium Supported on Alkaline Earth Metal Hydroxyapatites. *Catal Lett.* 145:668-78.
90. Dasireddy VDBC, Singh S, Friedrich HB. (2012). Oxidative dehydrogenation of *n*-octane using vanadium pentoxide-supported hydroxyapatite catalysts. *Appl Catal A.* 421-422:58-69.
91. Dasireddy VDBC, Friedrich HB, Singh S. (2013). Studies towards a mechanistic insight into the activation of *n*-octane using vanadium supported on alkaline earth metal hydroxyapatites. *Appl Catal A.* 467:142-53.
92. Dasireddy VDBC, Singh S, Friedrich HB. (2013). Activation of n-octane using vanadium oxide supported on alkaline earth hydroxyapatites. *Appl Catal A.* 456:105-17.
93. Sugiyama S, Osaka T, Ueno Y, Sotowa KI. (2008). Oxidative Dehydrogenation of Propane over Vanadate Catalysts Supported on Calcium and Strontium Hydroxyapatites *J Jpn Petrol Inst.* 51(1):50-7.
94. Sugiyama S, Sugimoto N, Hirata Y, Nakagawa K, Sotowa KI. (2008). Oxidative Dehydrogenation of Propane on Vanadate Catalysts Supported on Various Metal Hydroxyapatites. *Phosphorus Res Bull.* 22:13-6.
95. Sugiyama S, Shono T, Makino D, Moriga T, Hayashi H. (2003). Enhancement of the catalytic activities in propane oxidation and H–D exchangeability of hydroxyl groups by the incorporation with cobalt into strontium hydroxyapatite. *J Catal.* 214:8-14.
96. Khachani M, Kacimi M, Ensuque A, Piquemal JY, Connan C, Bozon-Verduraz F, et al. (2010). Iron–calcium–hydroxyapatite catalysts: Iron speciation and comparative performances in butan-2-ol conversion and propane oxidative dehydrogenation. *Appl Catal A.* 388:113-23.
97. El Kabouss K, Kacimi M, Ziyad M, Ammar S, Ensuque A, Piquemal JY, et al. (2006). Cobalt speciation in cobalt oxide-apatite materials: structure–properties relationship in catalytic oxidative dehydrogenation of ethane and butan-2-ol conversion. *J Mater Chem.* 16:2453-63.
98. Ehiro T, Misu H, Nitta S, Baba Y, Katoh M, Katou Y, et al. (2017). Effects of acidic-basic properties on catalytic activity for the oxidative dehydrogenation of isobutane on calcium phosphates, doped and undoped with chromium. *J Chem Eng Jpn.* 50(2):122-31.

99. Dasireddy VDBC, Singh S, Friedrich HB. (2014). Vanadium oxide supported on non-stoichiometric strontium hydroxyapatite catalysts for the oxidative dehydrogenation of *n*-octane. *J Mol Catal A*. 395:398-408.
100. Cortés Corberán V, Jia MJ, El-Haskouri J, Valenzuela RX, Beltrán-Porter D, Amorós P. (2004). Oxidative dehydrogenation of isobutane over Co-MCM-41 catalysts. *Catal Today*. 91-92:127-30.
101. Kim H, Park J, Park I, Jin K, Jerng SE, Kim SH, et al. (2015). Coordination tuning of cobalt phosphates towards efficient water oxidation catalyst. *Nat Commun.* 6(1):8253.
102. Yoon YS, Fujikawa N, Ueda W, Moro-oka Y, Lee KW. (1995). Propane oxidation over various metal molybdate catalysts *Catal Today.* 24:327-33.
103. Lee S, Halder A, Ferguson GA, Seifert S, Winans RE, Teschner D, et al. (2019). Subnanometer cobalt oxide clusters as selective low temperature oxidative dehydrogenation catalysts. *Nat Commun.* 10(1):954.
104. Sugiyama S, Hayashi H. (2003). Role of hydroxide groups in hydroxyapatite catalysis for the oxidative dehydrogenation of alkanes. *Int J Modern Physics B.* 17:1476-81.
105. Wei W, Moulijn JA, Mul G. (2009). FAPO and Fe-TUD-1: Promising catalysts for N_2O mediated selective oxidation of propane? *J Catal.* 262(1):1-8.
106. Ai M. (2003). Oxidation activity of iron phosphate and its characters. *Catal Today.* 85(2):193-8.
107. Jiménez-López A, Rodriguez-Castellón E, Maireles-Torres P, Diaz L, Mérida-Robles J. (2001). Chromium oxide supported on zirconium- and lanthanum-doped mesoporous silica for oxidative dehydrogenation of propane. *Appl Catal A*. 218:295-330.
108. Liu YM, Feng WL, Wang LC, Cao Y, Dai WL, He HY, et al. (2006). Chromium supported on mesocellular silica foam (MCF) for oxidative dehydrogenation of propane. *Catal Lett*. 106(3-4):145-52.
109. Cherian M, Rao MS, Hirt AM, Wachs IE, Deo G. (2002). Oxidative Dehydrogenation of Propane over Supported Chromia Catalysts: Influence of Oxide Supports and Chromia Loading. *J Catal.* 211(2):482-95.
110. Jibril BY. (2004). Propane oxidative dehydrogenation over chromium oxide-based catalysts. *Appl Catal A.* 264(2):193-202.
111. Mamedov EA, Vislovskii VP, Talyshinskii RM, Rizayev RG. (1992). Role of oxide catalysts basicity in selective oxidation. *Stud Surf Sci.* 72:379-86.
112. Klisinska A, Haras A, Samson K, Witko M, Grzybowska B. (2004). Effect of additives on properties of vanadia-based catalysts for oxidative dehydrogenation of propane. Experimental and quantum chemical studies. *J Mol Catal A*. 210:87-92.
113. Sugiyama S, Nitta E, Hayashi H, Moffat JB. (1999). Alkene selectivity enhancement in the oxidation of propane on calcium-based catalysts. *Catal Lett.* 59:67-72.

114. Sugiyama S, Nitta E, Hayashi H, Moffat JB. (2000). The oxidation of propane on nonstoichiometric calcium hydroxyapatites in the presence and absence of tetrachloromethane. *Appl Catal A.* 198:171-8.
115. Chizallet C, Bailly ML, Costentin G, Lauron-Pernot H, Krafft JM, Bazin P, et al. (2006). Thermodynamic Bronsted basicity of clean MgO surfaces determined by their deprotonation ability: Role of Mg^{2+}-O^{2-} pairs. *Catal Today.* 116(2):196-205.
116. Petitjean H, Krafft JM, Che M, Lauron Pernot H, Costentin G. (2010). Basic reactivity of CaO: investigating active surface sites under realistic conditions. *Phys Chem Chem Phys.* 12:14740 - 8
117. Sugiyama S, Moffat JB. (2002). Cation Effects in the Conversion of Methanol on Calcium, Strontium, Barium and Lead Hydroxyapatites. *Catal Lett.* 81(1-2):77-81.
118. Innovation in food engineering: new techniques and products, (2010). Passos M L, Ribeiro C P. Boca Raton, Florida: CRC Press. p. 87.
119. Thrane J, Mentzel UV, Thorhauge M, Høj M, Jensen AD. (2021). Hydroxyapatite supported molybdenum oxide catalyst for selective oxidation of methanol to formaldehyde: studies of industrial sized catalyst pellets. *Catal Sci Technol.* 11:970-83.